

W/PDC-TR-89-2044

AD-A211 319



## TWO DIMENSIONAL ORIFICE ARRAY, MONODISPERSE DROP SOURCE

John L. Dressler  
FLUID JET ASSOCIATES  
1216 Waterwyck Trail  
Spring Valley, Ohio 45370

February 1989

DTIC  
ELECTE  
AUG 15 1989  
S Q B D

Small Business Innovative Research

Phase I Final Report

Contract Number F33615-88-C-2865

Approved for Public Release; Distribution Unlimited

AERO PROPULSION AND POWER LABORATORY  
WRIGHT RESEARCH AND DEVELOPMENT CENTER  
AIR FORCE SYSTEMS COMMAND  
WRIGHT-PATTERSON AIR FORCE BASE OH 45433-6563

89

8

14


169

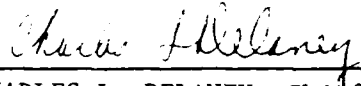
## NOTICE

When Government drawings, specifications, or other data are used for any purpose other than in connection with a definitely related Government procurement operation, the United States Government thereby incurs no responsibility nor any obligation whatsoever; and the fact that the government may have formulated, furnished, or in any way supplied the said drawings, specifications, or other data, is not to be regarded by implication or otherwise as in any manner licensing the holder or any other person or corporation, or conveying any rights or permission to manufacture, use, or sell any patented invention that may in any way be related thereto.

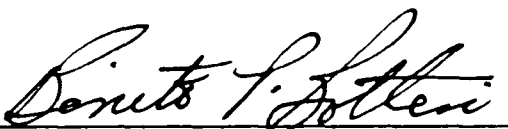
This report has been reviewed by the Office of Public Affairs (ASD/PA) and is releasable to the National Technical Information Service (NTIS). At NTIS, it will be available to the general public, including foreign nations.

This technical report has been reviewed and is approved for publication.

  
THOMAS A. JACKSON  
Project Engineer  
Fuels Branch

  
CHARLES L. DELANEY, Chief  
Fuels Branch  
Fuels and Lubrication Division  
Aero Propulsion and Power Laboratory

FOR THE COMMANDER

  
BENITO P. BOTTERI, Assistant Chief  
Fuels and Lubrication Division  
Aero Propulsion & Power Laboratory

"If your address has changed, if you wish to be removed from our mailing list, or if the addressee is no longer employed by your organization, please notify WRDC/POSF, Wright-Patterson AFB, Ohio 45433-6563 to help us maintain a current mailing list".

Copies of this report should not be returned unless return is required by security considerations, contractual obligations, or notice on a specific document.

REPORT DOCUMENTATION PAGE				Form Approved OMB No. 0704-0188	
1a. REPORT SECURITY CLASSIFICATION Unclassified			1b. RESTRICTIVE MARKINGS		
2a. SECURITY CLASSIFICATION AUTHORITY			3. DISTRIBUTION/AVAILABILITY OF REPORT Approved for public release. Distribution is unlimited.		
2b. DECLASSIFICATION/DOWNGRADING SCHEDULE					
4. PERFORMING ORGANIZATION REPORT NUMBER(S)			5. MONITORING ORGANIZATION REPORT NUMBER(S)		
6a. NAME OF PERFORMING ORGANIZATION Fluid Jet Associates		6b. OFFICE SYMBOL (if applicable)	7a. NAME OF MONITORING ORGANIZATION Aero Propulsion & Power Lab(WRDC/ POSF) Wright Research and Development Center		
6c. ADDRESS (City, State, and ZIP Code) 1216 Waterwyck Trail Spring Valley, Ohio 45370			7b. ADDRESS (City, State, and ZIP Code) Wright-Patterson AFB, OH 45433-6563		
8a. NAME OF FUNDING/SPONSORING ORGANIZATION Aero Propulsion & Power Lab		8b. OFFICE SYMBOL (if applicable) WRDC/ POSF	9. PROCUREMENT INSTRUMENT IDENTIFICATION NUMBER  F33615-88-C-2865		
8c. ADDRESS (City, State, and ZIP Code) Wright -Patterson AFB, OH 45433-6563			10. SOURCE OF FUNDING NUMBERS		
			PROGRAM ELEMENT NO. 65502F	PROJECT NO. 3005	TASK NO 21
11. TITLE (Include Security Classification)  TWO DIMENSIONAL ORIFICE ARRAY, MONODISPERSE DROP SOURCE					
12. PERSONAL AUTHOR(S) Dressler, John Lawrence					
13a. TYPE OF REPORT Final		13b. TIME COVERED FROM 6/27/88 TO 1/27/89		14. DATE OF REPORT (Year, Month, Day) 1989, February 10	
15. PAGE COUNT 37					
16. SUPPLEMENTARY NOTATION					
17. COSATI CODES			18. SUBJECT TERMS (Continue on reverse if necessary and identify by block number) monodisperse particles; droplets; sprayers; atomizers; jets; Rayleigh; ink jet; particle analyzers; combustors; fuel injection; liquid droplet radiators.		
FIELD	GROUP	SUB-GROUP			
21	02				
21	01				
19. ABSTRACT (Continue on reverse if necessary and identify by block number)  An acoustically driven drop generator has been constructed. It differs from other such devices in that it generates drops in a two-dimensional array. Further, the generator can break the liquid jets into uniformly-sized drops with diameters smaller than the minimum size predicted by Rayleigh's theory. One or two sizes of drops can be produced with diameters between 70 to 200 microns. The liquid jets are formed by liquid flowing from a constant pressure manifold through openings in a plate. The plate is made of laminated nickel and copper. Several plates with different hole patterns were constructed. The number of openings in the plates varied from 24 to 1010. The diameter of the openings ranged from 38 to 112 microns. A piezoelectric transducer creates pressure perturbations in the jets' velocity, forcing them to break into drops at the perturbation frequency. A signal generator provides one, two, or three sinusoidal signals for generating the input acoustic signal. A power amplifier boosts the signal and feeds it to the piezoelectric transducer. The jet breakup is observed and photographed through a microscope.					
20. DISTRIBUTION/AVAILABILITY OF ABSTRACT <input checked="" type="checkbox"/> UNCLASSIFIED/UNLIMITED <input checked="" type="checkbox"/> SAME AS RPT. <input type="checkbox"/> DTIC USERS			21. ABSTRACT SECURITY CLASSIFICATION Unclassified		
22a. NAME OF RESPONSIBLE INDIVIDUAL Thomas A. Jackson			22b. TELEPHONE (Include Area Code) (513)255-6462		22c. OFFICE SYMBOL WRDC/ POSF

# ABSTRACT

An acoustically driven drop generator has been constructed. It differs from other such devices in that it generates drops in a two-dimensional array. Further, the generator can break the liquid jets into uniformly-sized drops with diameters smaller than the minimum size predicted by Rayleigh's theory. One or two sizes of drops can be produced with diameters between 70 to 200 microns. The liquid jets are formed by liquid flowing from a constant pressure manifold through openings in a plate. The plate is made of laminated nickel and copper. Several plates with different hole patterns were constructed. The number of openings in the plates varied from 24 to 1010. The diameter of the openings ranged from 38 to 112 microns. A piezoelectric transducer creates pressure perturbations in the jets' velocity, forcing them to break into drops at the perturbation frequency. A signal generator provides one, two, or three sinusoidal signals for generating the input acoustic signal. A power amplifier boosts the signal and feeds it to the piezoelectric transducer. The jet breakup is observed and photographed through a microscope.



Accession For	
NTIS GRA&I	<input checked="" type="checkbox"/>
DTIC TAB	<input type="checkbox"/>
Unannounced	<input type="checkbox"/>
Justification	
By _____	
Distribution/	
Availability Codes	
Dist	Avail and/or Special
A-1	

## SUMMARY

1. Two-dimensional array nozzle plates were manufactured and operated. Square and circular drop sources as well as line sources were made.
2. Instabilities on the liquid jet, that were dependent on the amplitude of the stimulation signal, were observed at wavelengths shorter than the jet's circumference. Small perturbations at these wavelengths were shown to be stable as predicted by Rayleigh's theory. When the stimulation amplitude was increased, the perturbations became unstable and the jets broke into drops at the frequency of the applied stimulation.
3. By using high acoustic power, we increased the highest unstable frequency for jet breakup by almost 50 percent. For a jet of a particular diameter, we produced drops with a volume only two-thirds of the previously accepted minimum volume.
4. We increased the drop velocity by increasing the acoustic power. This allowed us to change the drop spacing, and therefore the drop number density, without changing the drop diameter or production frequency.
5. Acoustic pumping was used to make drops from an array of nozzles. The liquid pressure in the fluid manifold was set so jets did not form at the nozzles. The acoustic signal was used to pump energy into the liquid and eject drops from the nozzles. The drop production was started and stopped by turning the acoustic signal on and off.
6. We produced nozzles that were slots rather than circles and made sheets of liquid. These sheets were partially broken into drops by the application of high power acoustic stimulation.

## TABLE OF CONTENTS

Abstract	1
Summary	2
Table of Contents	3
List of Figures	4
1. Introduction	5
2. Equipment	7
2.1 Droplet Generator Description	7
2.2 Nozzle Plate Descriptions	8
2.2.1 Linear Array Nozzle Plate	8
2.2.2 Circular Array Nozzle Plate	8
2.2.3 Concentric Circle Array Nozzle Plate	9
2.2.4 Rectangular Array Nozzle Plate	9
2.2.5 Slotted Nozzle Plate	9
3. Test Results	10
3.1 Linear Array Nozzle Plate	10
3.2 Circular Array Nozzle Plate	11
3.3 Concentric Circle Array Nozzle Plate	11
3.4 Rectangular Array Nozzle Plate	12
3.5 Drop Spacing Dependence on Stimulation Amplitude	12
3.6 Amplitude Dependent Jet Instabilities	13
3.7 Viscous Fluid Experiments	14
3.8 Experiments With Fluid Sheets	14
3.9 Acoustically Pumped Drop Streams	15
4. Potential Applications	15
5. References	16
Figures	17

## LIST OF FIGURES

1.	Droplet Generating Apparatus	17
2.	WPAFB-131-C1 Drop Generator, Circular Array, 30 Jets, 70 micron drops	18
3.	WPAFB-131-C2 Drop Generator, Array of Four Concentric Circles, 117 jets with 70 micron drops and 96 jets with 210 micron drops	19
4.	Contact Prints of Orifice Plates	20
5a.	Linear Array, 24 holes, 64 microns	21
5b.	Circular Array, 30 holes, 38 microns	21
5c.	Concentric Circular Array, 117 holes - 38 microns, 96 holes - 114 microns	22
5d.	Rectangular Array, 112 holes - 76 microns	23
5e.	Slots, 50.8 microns average width, 6350 microns long	23
6a.	Linear Array positioned radially from stimulator	24
6b.	Graphical representation of filament lengths shown in the photo above.	24
7.	Circular Drop Array, 30 jets - 70 micron drops, Composite Photo	25
8.	Array of Four Concentric Circles, 117 jets with 70 micron drops, 96 jets with 120 micron drops.	26
9.	Rectangular Array, 112 jets - 150 micron drops	26
10.	Typical Rayleigh Breakup, 17.9 kHz	27
11.	Increased Droplet Spacing due to high amplitude stimulation, 17.9 kHz	28
12.	Amplitude Dependent Instabilities, 30.4 kHz	29
13a.	Low Amplitude Stimulation, 43.9 kHz, Stable Jets	29
13b.	High Amplitude Stimulation, 43.9 kHz, Unstable Jets	29
14.	Droplet Spacing Stretching - 10 cP fluid	30
14a.	Low amplitude stimulation, 15.4 kHz	30
14b.	Medium amplitude stimulation, 15.4 kHz	30
14c.	High amplitude stimulation, 15.4 kHz	30
15.	Amplitude dependent instability - 10 cP fluid, 25.9 kHz	30
16a.	Fluid sheet with spatial perturbations	31
16b.	Fluid sheet with spatial perturbations and sinusoidal velocity perturbations. 12.66 kHz	31
16c.	Fluid sheet with spatial perturbations and sinusoidal velocity perturbations. 5.46 kHz	32
16d.	Fluid sheet with spatial perturbations and sinusoidal velocity perturbations. 2.50 kHz	32
16e.	Fluid sheet with spatial perturbations and square-wave velocity perturbations. 5.5 kHz	33
16f.	Fluid sheet with spatial perturbations and square-wave velocity perturbations. Higher amplitude, 5.5 kHz	33
16g.	Fluid sheet with spatial perturbations and square-wave velocity perturbations. 5.0 kHz	34
17.	Acoustically Pumped Drop Streams - 10 cP Fluid	35
17a.	Low amplitude stimulation	35
17b.	High amplitude stimulation	35

## A TWO DIMENSIONAL HIGH POWER ACOUSTIC DROPLET GENERATOR

### 1. INTRODUCTION

The purpose of this effort is to develop a versatile, highly precise, controllable, two-dimensional droplet generator. In reaching this goal two objectives were to be met in Phase I. First, multi-droplet generators, producing droplets in a rectangular array and in an axisymmetric array, were to be designed and constructed. Second, control over the characteristics of the acoustic wave, used to drive the droplet formation process, was to be established for a variety of droplet patterns. We have worked on both types of acoustic drop generators: the continuous-jet and the drop-on-demand.

Continuous-jet acoustic drop generators are a type of droplet generator that breaks a liquid jet into a stream of drops by means of an acoustic signal. The acoustic signal, called the stimulation, makes velocity perturbations on the jet. The jet then breaks into drops at the acoustic signal's frequency. This process for droplet formation was first described mathematically by Rayleigh[1] and is generally referred to as Rayleigh breakup. These drop generators are commercially available with a single jet[2] or with multiple jets arranged along one line[3]. The single jet devices can be called point drop sources and the multiple jet devices can be referred to as line drop sources. These generators are noted for producing drops with extremely uniform diameters and spacings. Consequently they are used in applications such as ink jet printing[4] where drop diameters and trajectories must be controlled precisely.

The second type of acoustic drop generator, called drop-on-demand, does not have a continuous liquid jet. It produces a liquid drop only when a piezoelectric transducer is driven with a high voltage pulse. The advantage of these drop generators is that, independently of the drop diameter, their drop spacing can be varied over wide limits by changing the pulse frequency. They are used for low volume printing applications.

The type of droplet generator that we hope to replace for some applications is the air blast atomizer. This atomizer produces droplets by tearing a sheet of liquid apart with the shear force of high velocity air. Air blast atomizers produce high volumes of droplets with a wide spectrum of diameters and spacings. The spray forms a cone of drops that originates at the nozzle. A significant problem with this type of sprayer is the mass flux is not spatially uniform. Air blast atomizers are used for high volume applications such as spraying fuels into combustors, painting automobiles, and for creating agricultural sprays.

We are attempting to remove limitations to more uses for acoustic drop generators by making design improvements. The



biggest limitation to additional uses of continuous-jet acoustic drop generators is their low flow rate. The flow rate is approximately one milliliter per minute per jet so the available units have flow rates of less than fifty milliliters per minute. A second problem is the limitation on drop diameter made by Rayleigh's theory of jet breakup. According to his theory, the smallest drop diameter that can be made is 1.68 times the jet diameter. Therefore, to make small drops, the jets must also be small and consequently there will be problems with dirt plugging the nozzles. A third limitation is that the drop spacing and the drop number density are related to the acoustic frequency, which is directly related to the drop diameter. It is therefore impossible to obtain many desired experimental conditions because the drop number density and the drop diameter can not be varied independently.

To increase the volume of produced drops, our drop generator contains nozzles arranged in two dimensional arrays. With these nozzle arrays, the drop generator has larger numbers of nozzles than the currently available commercial units. The nozzle plates were made by a photofabrication process and we demonstrated that it was possible to produce large numbers of nozzles with tightly controlled diameters, located in two-dimensional patterns.

We also constructed the drop generator so a broader range of drops and an expanded range for drop spacing can be made from each nozzle diameter. Dressler[5] had predicted that Rayleigh's limits for unstable jet wavelength are not applicable if large acoustic signals are applied to the jets. Further, he also predicted that the drop velocity and the drop spacing can be controlled by varying the amplitude of the acoustic signal. The drop generator contains a high power acoustic source so these predicted effects on drop diameter and spacing can be made.

The drop generator was operated in the drop-on-demand mode. We demonstrated that one transducer could be used to form drops from an array of nozzles. The pressure in the liquid manifold was reduced so there was no steady flow through the nozzles. The piezoelectric transducer was driven at one of its resonant frequencies and drops were simultaneously produced from some of the nozzles at the driving frequency.

Breaking a liquid sheet into drops with an acoustic signal is another method tested to increase the volume produced by the drop generator. Dressler[6] has shown that, due to surface tension, a liquid sheet is stable at all wavelengths for small amplitude perturbations. With this drop generator, we have shown that a circular liquid jet, which is stable for small perturbations at some wavelengths, can still be broken up at these wavelengths by the application of a large acoustic signal. Based on this result, the analogous technique of breaking a stable liquid sheet into drops by applying a high powered acoustic signal was tested. Partial success was achieved when a portion of the sheet broke into drops at the acoustic frequency.

## 2. EQUIPMENT

### 2.1 DROPLET GENERATOR DESCRIPTION

Figure 1 is a photograph of the drop generator along with the other equipment needed for its operation. The streams of drops flowing from the generator appear as an array of white vertical lines against the black background. On the right side of the picture is the electronics rack. The acoustic power amplifier is in the rack bottom and a function generator is sitting on the amplifier. At the rack top is a panel containing the stroboscope synchronization circuit, the transducer matching transformer, and the Stimulation Waveform Generator. To the right of the rack is the fluid supply tank and its pressure regulator. The microscope, on the left side of the photograph, is on a boom stand for easy positioning along the jet array and it has a 35 mm camera attachment.

Compressed air forces liquid from the supply tank to the drop generator where a pressure gauge, located on the manifold, monitors the static pressure of the fluid adjacent to the orifice plate. Controlling the manifold pressure adjusts the flow of liquid through the orifices.

There are two filters in the fluid line between the fluid supply tank and the drop generator head. The filter close to the supply tank has a porosity of .8 microns and the one attached to the drop generator has a porosity of 2 microns. These filters remove dirt particles from the fluid that may plug the orifices. An exhaust valve located in the exhaust fitting of the drop generator head allows filtered fluid to be flushed through the manifold. Flushing the manifold before starting the drop generator helps to prevent dirt from blocking the orifices. The exhaust valve is closed during normal operation.

The stimulation system includes the function generator, the Stimulation Waveform Synthesizer, the Denon power amplifier, the matching transformer, and the piezoelectric transducer. This system drives the sausage mode of the jet's radial perturbation. This perturbation, which was called the varicose mode by Rayleigh, is symmetrical around the axis of the jet and varies sinusoidally along the jet's axis. The function generator provides a variable clock signal for the synthesizer and the synchronizer. The Stimulation Waveform Synthesizer generates up to three arbitrary waveforms that can be added together, with variable weighting. The composite signal is then amplified by the Denon power amplifier and sent through a matching transformer to the piezoelectric transducer. The piezoelectric transducer generates pressure variations in the fluid manifold which make velocity perturbations on the liquid jets. If the jet is unstable at the wavelength and amplitude of the velocity perturbations, it breaks into drops at the frequency of the stimulation signal. Since the nozzle plates used for this project contain one or two different jet diameters, the Stimulation Waveform Synthesizer must be able to generate a signal that contains a separate frequency for each jet diameter. When a single frequency stimulation is desired, the function

generator can be used to drive the power amplifier directly.

A stroboscope and synchronizing circuit are included with the drop generator. The high speed light flashes in synchronism with the stimulation signals and creates a stationary image of the drop formation process for viewing or photographing.

Figure 2 and Figure 3 are photographs of the operating drop generator head. A fluid manifold is machined in a plastic block and the top of the manifold is sealed with a brass plate. The nozzle plate covers the lower opening to the fluid manifold. fluid connections are made in two sides of the manifold. A rod from the piezoelectric transducer goes through a hole in the top plate, crosses the fluid manifold, and directly contacts the nozzle plate.

Figure 2 shows a monodisperse spray being made from a nozzle plate containing a circular array of nozzles with equal diameters. The nozzle plate used in Figure 3 contains nozzles of two different diameters and the spray contains droplets of two sizes.

The fluid used for most of the experiments is distilled water with added buffers, corrosion inhibitors, and germicide. For a few experiments, the viscosity of the fluid was increased to 10 cP by using glycerol.

## 2.2 NOZZLE PLATE DESCRIPTIONS

Several configurations of nozzle plates were fabricated. The plates are formed by a process developed to make exposure masks for printed circuits. These plates are made of laminations of nickel and copper and hole patterns of almost any shape can be placed in the mask.

The images in Figure 4a-4e were made by placing the nozzle plates on photographic paper and making a contact print. These photographs show the nozzles as dark spots inside the nozzle plate boundary.

The nozzle plates were then placed in a photographic enlarger and the nozzle arrays were projected onto photographic paper. The images in Figure 5a-5e are the projected images and they are approximately a 4.5X magnification of the nozzle images of Figure 4.

### 2.2.1 LINEAR ARRAY NOZZLE PLATE

Figures 4a and 5a are the images of the nozzle plate where the nozzles are arranged on a line that passes through the center of the nozzle plate. The nozzles are 64 microns (.0025 in.) in diameter and there is a space of .050 in. (1.27 cm) between nozzles. The middle three nozzles were omitted from the array because the piezoelectric transducer touches the nozzle plate's center. This pattern is used to study the flexing amplitudes on the nozzle plate. This pattern is also used for photographing jet instabilities without the clutter of too many jets.

### 2.2.2 CIRCULAR ARRAY NOZZLE PLATE

Figures 4b and 5b are the images of a circular array of nozzles. This plate has thirty holes, with a diameter of 38 microns, evenly spaced on a circle of .5 in. (1.27 cm) diameter.

This plate produces an axisymmetric flow of monodisperse drops.

#### 2.2.3 CONCENTRIC CIRCLE ARRAY NOZZLE PLATE

Figures 4c and 5c are the images for a nozzle plate that contains nozzles located on four concentric rings. The nozzles on the first and third rings, counting from the center, are of 114 microns diameter and the nozzles on the second and fourth rings are of 38 microns diameter. The diameters of the nozzle circles are .3, .4, .5, and .6 in. (.76, 1.02, 1.27, and 1.52 cm). This plate forms an axisymmetric spray that consists of drops of two distinct diameters.

#### 2.2.4 RECTANGULAR ARRAY NOZZLE PLATE

Figures 4d and 5d are the images for a square array of jets. This pattern was made to create a high density drop spray from a two dimensional source. There are 112 nozzles, with diameters of 76 microns, in this array and .050 in. (.127 cm) is the grid spacing.

#### 2.2.5 SLOTTED NOZZLE PLATE

Figures 4e and 5e show a nozzle plate that has openings that are slots rather than circles. This nozzle plate forms sheets of liquid and it is used to study the stability of sheets of liquid with high amplitude stimulation. The slots are each 6350 microns long (.25 inch) and the average width is 50.8 microns (.002 inch). They are spaced 1.27 centimeters apart.

### 3. TEST RESULTS

#### 3.1 LINEAR ARRAY NOZZLE PLATE

Figure 6a is a photograph of drop streams produced by the linear array nozzle plate. Twelve of the twenty four streams are shown. Referring to Fig 4a, they are the jets on one side of the center of the plate. The piezoelectric transducer drives the nozzle plate on the left of the jets in Fig. 6a and the plate is bonded to its holder on the right of the figure. The other twelve jets in this array, are located symmetrically on the other side of the stimulator tip.

This nozzle plate is mounted in a circular holder by gluing the outer edge of the plate to the nozzle plate holder. This ring holds the plate against the pressure of the liquid in the manifold and establishes the boundary conditions for the vibrations of the orifice plate.

The orifice plate is driven in the center by a piezoelectric transducer. The vibrations radiate from this point and are reflected off the glued boundary. The radiated and reflected waves create a standing wave on the orifice plate. The glued plate boundary can also absorb a portion of the acoustic energy radiated from the transducer. The ratio of the absorbed to reflected energy determines the standing wave ratio which is an indication of the ratio of the peaks and nodes of the vibration amplitude on the plate.

The standing wave pattern can have a profound effect on the drop production if the jets are being stimulated at a frequency where the jet instability is amplitude dependent. If a jet originates at a point of minimum vibration amplitude, then possibly it may not receive enough stimulation energy to break into drops at the desired frequency.

It is difficult to mathematically determine the shape of the standing wave because the boundary conditions at the point of excitation and at the plate boundary are not known. The velocity of the flexing waves is also difficult to calculate because the plate is laminated and perforated by the nozzles.

Because the standing wave can not be determined mathematically, the linear orifice array was fabricated to provide a visual method for observing the vibrational standing wave.

When a jet is stimulated at an unstable wavelength, the perturbation grows until it breaks the jet into drops. The time required for the perturbations to grow enough to break the jet is called the breakup time. The distance the jet travels before it breaks is called the filament length, which is the length of the unbroken jet filament extending from the orifice plate. This distance is related to the instability's growth rate and initial amplitude. Since the standing wave on the nozzle plate excites all the jets at the same frequency, the jets all have the same diameter and the initial perturbations are kept small, the growth rate of the instability on each jet should be the same. The filament lengths of the jets are therefore related to the amplitude of the vibrations on the nozzle plate.

Figure 6b is a graphical representation of the filament lengths of the jets shown in Figure 6a and is a representation of the amplitude of the standing wave pattern on the nozzle plate. The shortest jet filaments represent large amplitude vibrations of the plate while long jet filaments occur where the vibrational amplitude is small.

The jet disturbance grows in an exponential manner and therefore the difference in filament lengths is related to the logarithm of the plate vibrational amplitudes. Since the logarithm varies slower than the original stimulation amplitude, the variations in the plate vibrations are much larger than the filament length variations. A graph of the plate vibrations would therefore have much larger variations than the profile of the filament lengths shown in Figure 6b.

Using the jet filament data does not provide all the information required to determine the standing wave on the nozzle plate. When standing wave patterns are made, it is necessary to determine which sections of the pattern are moving in phase and which sections are moving out of phase. The filament length measurements provide only amplitude information; they do not provide the phase information.

### 3.2 CIRCULAR ARRAY NOZZLE PLATE

A photograph of the drop streams produced with the circular array nozzle plate is shown in Figure 7. This is two separate photographs spliced together to get the view of one side of this array. The center jets are in focus and the jets on the edges of the array move farther from the camera and out of focus. The jets on the far side of the array are not visible.

These jets are located equidistant from the piezoelectric transducer tip and therefore the amplitude of the plate vibration is almost constant at the nozzles. The large variations in filament length, displayed by the linear jet array, are not present with this circular array.

### 3.3 CONCENTRIC CIRCLE ARRAY NOZZLE PLATE

Figure 8 shows a photograph of the drop streams produced by a nozzle plate containing nozzles of two different diameters, located on concentric circles. Figures 4c and 5c show the hole placement for this plate.

Since the nozzles are located on circles, it is not possible to get many of the jets in focus at the same time. The microscope was set to get some drops of each diameter in focus.

The breakup of two different jet diameters into drops requires that the nozzle plate be vibrated at two separate frequencies, and we expected to create two standing waves on the plate, one at each frequency. The nozzles are arranged on circles equidistant from the transducer tip and we expected the standing waves on the nozzle plate to be azimuthally constant. Therefore all the jets emerging from nozzles on the same circle should have almost equal filament lengths.

In Figure 8, the filaments for the large jets, originating in the same circle of nozzles, are not the same length. This shows that the standing wave, driving the large jets, is not

constant at points equidistant from the transducer tip as we expected. The reason for the nonuniform vibrations is not understood at this time.

### 3.4 RECTANGULAR ARRAY NOZZLE PLATE

Figure 9 is a photograph of a section of the drop array produced with the nozzle plate shown in Figures 4d and 5d. This photograph was made with one row of the jets in focus and the rows farther from the camera out of focus.

The rows of nozzles are not equidistant from the piezoelectric driver and therefore the filament lengths for these jets are not expected to be equal.

The rectangular nozzle plate produces a higher concentration of drops than the linear or axisymmetric designs.

### 3.5 DROP SPACING DEPENDENCE ON STIMULATION AMPLITUDE

Dressler[4] has derived a formula for the velocity of a drop that is produced by the acoustic breakup of a liquid jet. This equation is different from other equations in that it includes the stimulation amplitude as a variable. The formula is repeated here without derivation and it is

$$v_d = v_j \left( 1 - \frac{T}{\rho R_j v_j^2} \right) + \frac{v_s^2}{2v_j}$$

where  $v_d$  is the drop velocity,  $v_s$  is the stimulation velocity,  $v_j$  is the jet velocity,  $\rho$  is the liquid density,  $T$  is the surface tension, and  $R_j$  is the jet radius.

This formula shows that increasing the stimulation amplitude increases the drop velocity and consequently the drop spacing also increases.

Figures 10 and 11 are photographs of an experiment to determine if the drop spacing could be increased by increasing the stimulation amplitude.

Figure 10 shows a photograph of the jet and drop array produced with the linear array nozzle plate. This plate was used because of the large variations in stimulation amplitude that exist along the row of nozzles. The transducer is located at the left of the array and the row of nozzles extends radially from the transducer tip. The left jets are closer to the stimulator and have a larger stimulation amplitude than the right jets, which are farther from the transducer.

Figure 10 is a photograph of what can be called Rayleigh breakup. The amplitude of the stimulation is low and the wavelength of the stimulation is longer than the circumference of the jet. The frequency of the stimulation is 17.9 kHz.

The power to the transducer was increased dramatically and Figure 11 is a photograph of the results. The drops from the jets on the left of the photograph are spaced farther apart than the drops from the jets on the right of the photograph. All the jets in the photograph are being driven, and broken into drops, at the same frequency of 17.9 kHz. The drop spacing variations are due to the drop velocity differences, caused by the

stimulation amplitude variation from the left to the right side of the jet array.

In Figures 10 and 11, the drops on the right of both photographs have approximately the same spacing. This indicates that where the stimulation amplitude is low, the drop velocity is determined mainly by the jet velocity. When the drop spacings on the left of the photographs are compared, the drops with the higher stimulation amplitude have the higher drop velocity and spacing. This also shows that a high stimulation velocity is required to make a noticeable change in the drop velocity.

### 3.6 AMPLITUDE DEPENDENT JET INSTABILITIES

Rayleigh developed a theory of jet breakup that was based on the study of infinitesimal perturbations. He derived a limit on the wavelength for unstable perturbations and determined that perturbations with wavelengths less than the jets circumference were stable. This stability limit restricts the diameter of the smallest drop that can be produced to 1.68 times the jet diameter.

We have exceeded Rayleigh's limit on stable wavelengths by using high amplitude stimulation. By supplying energy to the drop formation process with high amplitude stimulation, we provide the energy required to form the surface that is made when the drops form.

Rayleigh's theory for small amplitude perturbations has been experimentally verified and small perturbations, of wavelength shorter than the jet's circumference, are stable. When we apply large perturbations with the same wavelength to the jet, it can break into drops. Because there is a critical amplitude that must be exceeded to get instability, we call these amplitude dependent instabilities.

Figure 12 is a photograph that shows the amplitude dependent instabilities on jets formed with the linear array nozzle plate. The stimulation frequency is 30.4 kHz. which is slightly higher than the limit derived by Rayleigh for unstable perturbations. This plate was used because the stimulation amplitude varies from jet to jet due to the standing wave pattern of the nozzle plate's vibration. The jets have the same diameter, velocity, and stimulation frequency.

The two middle jets have a lower amplitude stimulation and they are stable. The photograph clearly shows that the jet perturbations decay as the jet travels from top to bottom of the figure.

The two outside jets of Figure 12 are unstable and form drops. These jets have a larger stimulation amplitude than the two inner jets. The jet diameters and velocities are equal, and the stimulation frequency is the same for all jets.

Figures 13a and 13b show the same jets with the stimulation frequency increased to 43.9 kHz. This frequency produces perturbation wavelengths that are much shorter than Rayleigh's shortest unstable wavelength. In Figure 13a, the stimulation amplitude is not high enough to cause instabilities and the perturbations on the jets decay. The stimulation amplitude is increased and three of the jets become unstable in Figure 13b.



Because of the nonuniform stimulation, two of the jets do not have sufficient stimulation and they are stable.

Figures 12 and 13 show that jets which are stable for small perturbations at 30.4 kHz can be uniformly broken into drops at 43.9 kHz. if the stimulation amplitude is large.

### 3.7 VISCOUS FLUID EXPERIMENTS

In the theoretical explanations of the drop velocity and jet stability dependence on stimulation amplitude, Dressler[5] assumed the possible effects of fluid viscosity were not significant and did not consider viscosity in the calculations. As a test of that assumption, the relevant experiments were repeated with a fluid of viscosity of 10 cP to determine if there was any qualitative change in the results.

Figures 14a, 14b, and 14c were made to see if there was any qualitative change in the droplet velocity modulation if the fluid viscosity was increased to 10 cP. As this series of photographs shows, increasing the stimulation amplitude increases the drop spacing, in a manner similar to that seen with 1 cP fluid.

Figure 15 is a photograph of the amplitude dependent instabilities using a fluid with viscosity of 10 cP. This test was made to determine if an increase in viscosity would make any dramatic changes in the amplitude dependent instabilities and we saw none.

### 3.8 EXPERIMENTS WITH FLUID SHEETS

Sheets of fluid are stable for small perturbations of all wavelengths due to the effects of surface tension. We conducted experiments on fluid sheets to determine if they could be made to break into tubes or drops due to the effect of a large stimulation signal.

Figures 16a-16g show the results of some of our efforts. We were not able to break the entire sheet into drops but we did have some success in forming uniform drops from a portion of the sheet.

Figure 16a shows the sheet formed by the nozzle plates of Figures 4e and 5e. The slot had a square-wave pattern of period 500 microns in its thickness, which made spatial perturbations in the fluid sheet thickness. These thickness perturbations are visible in the sheet as vertical striations.

Sinusoidal stimulation at 12.66 kHz, 5.46 kHz, and 2.50 kHz was applied to the fluid sheet and the photographs of Figures 16b-16d were made. These photographs show the perturbations due to the stimulation as horizontal striations. There is no evidence here that the perturbations were unstable.

Square wave stimulation at 5.5 kHz. and 5.0 kHz was used and the photographs of Figures 16e-16g were made. These photographs show that one edge of the sheet has become unstable and it forms a tube which then ejects a drop. In Figure 16f the stimulation amplitude was increased from Figure 16e, causing drops to be formed. This demonstrates the amplitude dependent nature of the drop formation process.

Figure 16g was made with square wave stimulation at 5.0 kHz.

With these conditions, tubes formed but there was no drop formation at the end of the tube.

The stimulation signal was made as large as our equipment could provide and the drops of Figure 16f were the best that were made. From these experiments, it looks as if a large stimulation signal may break the sheet into drops. However, we did not have the capability to make the required stimulation amplitude.

### 3.9 ACOUSTICALLY PUMPED DROP STREAMS

Drop-on-demand drop generators[7] create one drop of liquid when they are driven by a high voltage pulse. The voltage pulse drives a piezoelectric transducer which decreases the volume in a fluid chamber and ejects a drop through an opening in the chamber wall. This type of drop generator does not form a continuous stream of drops. It produces a drop only when it receives the command.

Drop-on-demand drop generators have lower drop production rates and lower drop diameter precision than continuous jet devices have. Their advantage is that the drop stream can be switched on or off easily.

We tested the drop generator to determine if arrays of drops could be produced by pulsing the stimulation transducer. The fluid supply valve was shut and the exit port of the fluid manifold was opened. The tube from the manifold exit to a collection beaker created a syphon and the pressure in the manifold was slightly negative.

The stimulation was turned to a high level and the photograph of Figure 17a was made. The jets closest to the stimulator tip were producing drops at 15 kHz., the frequency of the stimulation. The stimulation amplitude was increased, and more of the nozzles in the array started to produce drops. The higher drop production can be seen in Figure 17b.

The nozzle plate used here was the linear array plate. This plate does not have uniform stimulation across the nozzle array and that explains why the jets closest to the stimulator produced drops at the lower stimulation amplitude. When the stimulation amplitude was increased, nozzles farther from the stimulator tip received enough energy to produce drops. When the stimulation was turned off, the drop production stopped.

The drop frequency produced by this acoustic pumping, 15 kHz., is extremely high for a drop-on-demand generator. We will have to make further tests to see if the drop rate can be varied continuously from lower values to 15 kHz.

## 4. POTENTIAL APPLICATIONS

The development of two-dimensional monodisperse drop generators will find applications where spatially uniform sprays are needed and where large flow monodisperse flows are needed.

Monodisperse drop generators are now used as calibration tools for particle analyzers. The development of two-dimensional devices has expanded their capabilities and they now can provide sprays with a spatially controlled number density as well as controlled diameters. These devices will provide a means to calibrate particle analyzers with a known level of obscuration.

Large monodisperse droplet generators can find uses in combustion studies. Droplets can be generated at reasonable rates and with a high degree of control over the droplet initial conditions (size, velocity, and number density).

The development of the technique for breaking jets into drops with diameters that are smaller than have been obtained previously will give the drop generators wider flexibility for both combustion and calibration uses. The development of the technique for changing drop spacing with the acoustic signal will expand the capabilities of acoustic drop generators that are used as calibration devices for particle analyzers.

The Liquid Drop Radiator Project[8] and aircraft icing studies are two additional areas where the large-flow two-dimensional drop generators developed in this project may be used.

## 5. REFERENCES

1. J.W.S. Rayleigh, "On the Instability of Jets", Proceedings of the London Mathematical Society, Vol. 10, p 4 (1878). Available in U.S. in S. Chandrasekhar, Hydrodynamic and Hydromagnetic Stability, Chapter 12, Oxford University Press, London, 1961
2. Lars Strom, "The Generation of Monodisperse Aerosols by Means of a Disintegrated Jet of Liquid," Review of Scientific Instruments, Vol 40, No. 6, June 1969, pp 778-782
3. J.L. Dressler and G.O Kraemer, "A Multiple Species Drop Generator for Calibration of a Phase Doppler Particle Analyzer," 2nd American Society for Testing and Materials Symposium on Liquid Particle Sizing Techniques, Nov. 9-11, 1988, Atlanta, Georgia
4. P.L. Duffield, "DIJIT Ink Jet Printing," Proceedings Technical Association of the Graphic Arts, 1974, pp. 116-132
5. J.L. Dressler, "Shock Model of Liquid Jet Breakup," Lawrence Livermore National Laboratory, UCRL-78480, Rev. 1, Oct 20, 1976
6. J.L. Dressler, "Active Electromechanical Control of Fourth-Order Continua," Master of Science Thesis, MIT, Cambridge, MA, May 1966
7. Kyser, E.L., Collins, L.F., and Herbert, N., "Design of an Impulse Ink Jet," Journal of Applied Photographic Engineering, Vol. 7, NO. 3, June 1981, pp 73-79
8. Presler, A.F., Coles, C.E., Diem-Kirsop, P.S., and White, K.A., "Liquid Droplet Radiator Program at the NASA Lewis Research Center," American Institute of Aeronautics and Astronautics/American Society of Mechanical Engineers Thermophysics and Heat Transfer Conference, "86-HT-15, Boston, MA, 1986



FIGURE 1. Droplet Generating Apparatus.

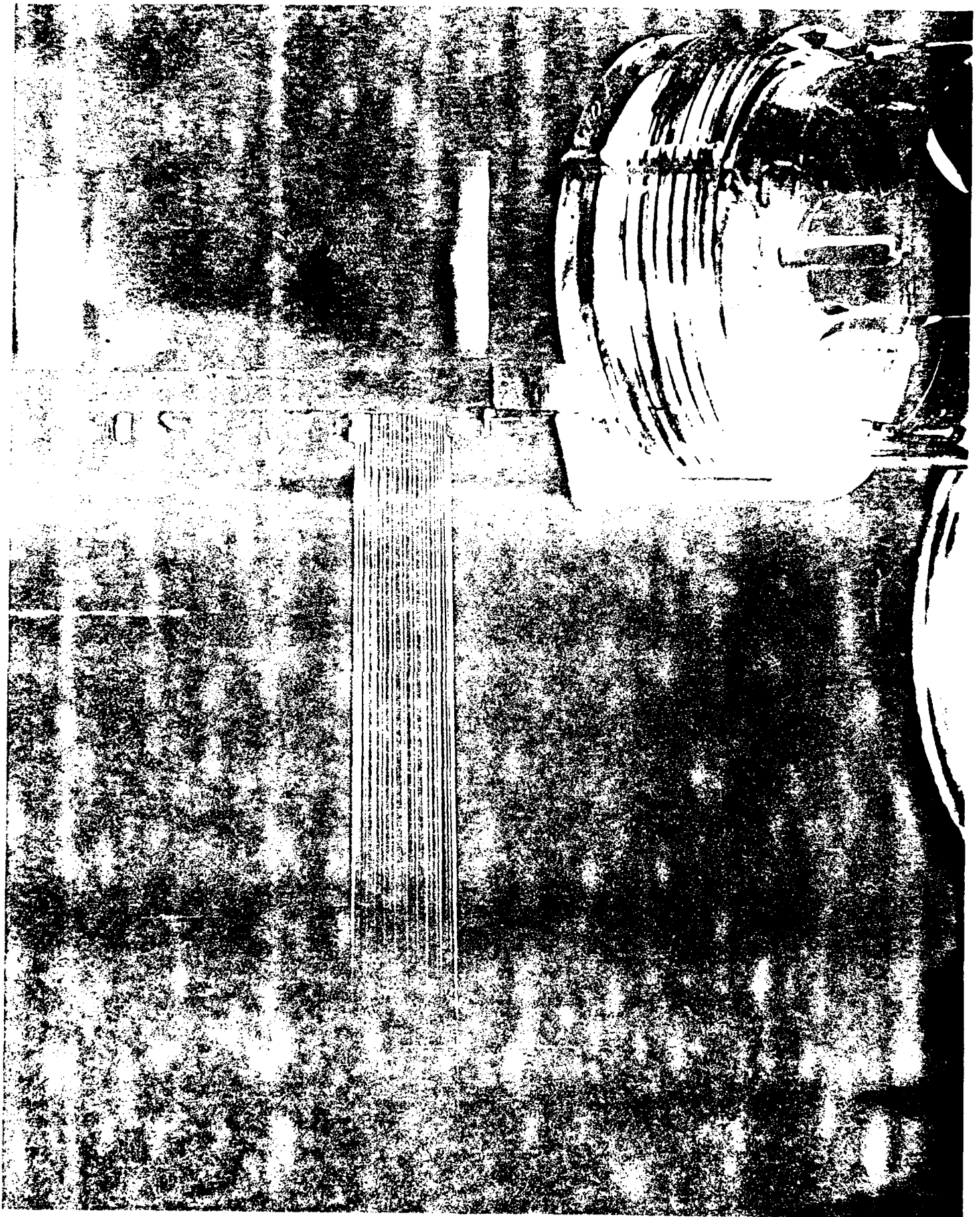


FIGURE 2. WPAFB-131-C1 Drop Generator.  
Circular Array. 30 jets. 70 micron drops.

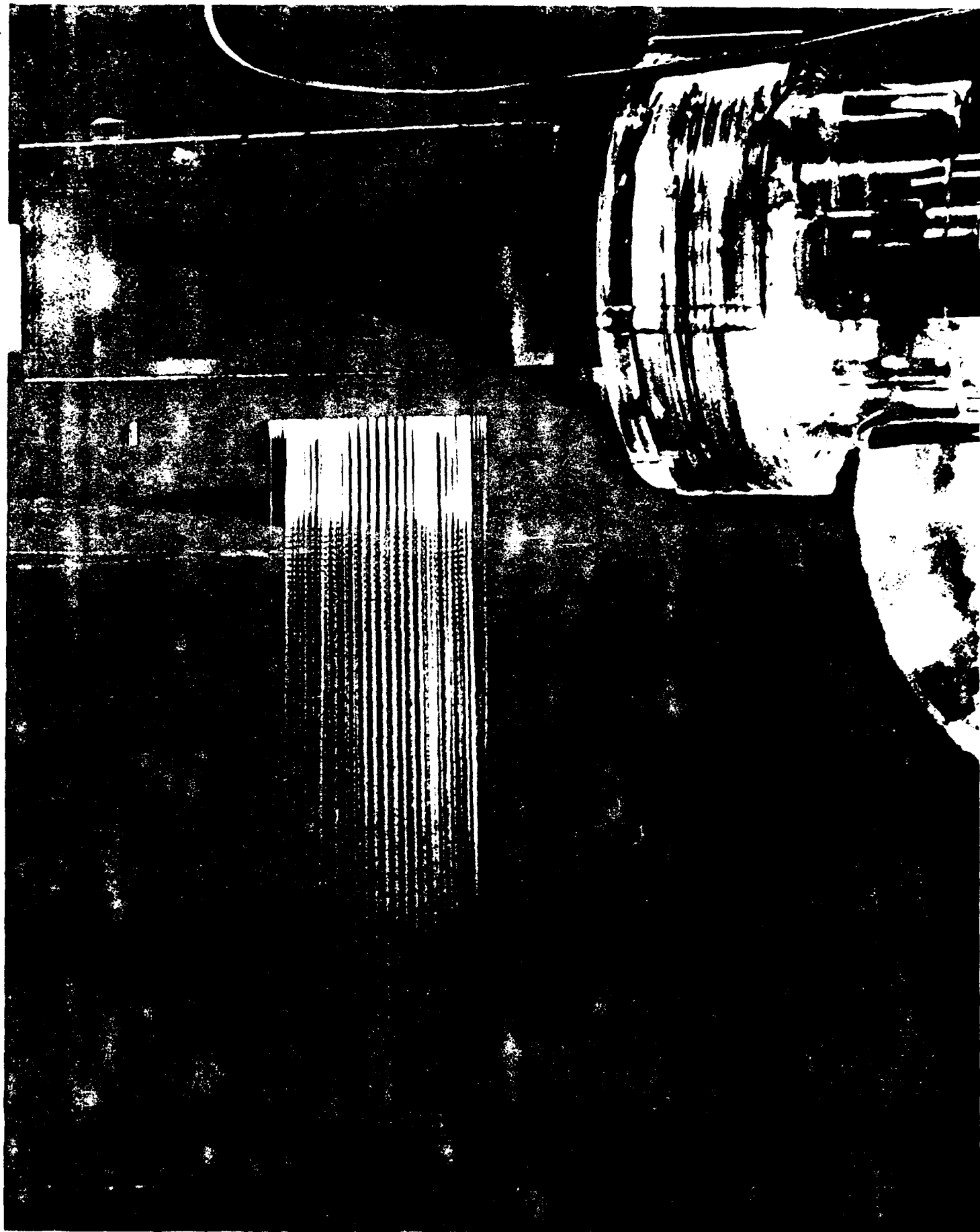


FIGURE 3. WPAFB-131-C2 Drop Generator.  
Array of 4 concentric circles.  
117 jets with 70 micron drops & 96 jets with 210 micron drops.

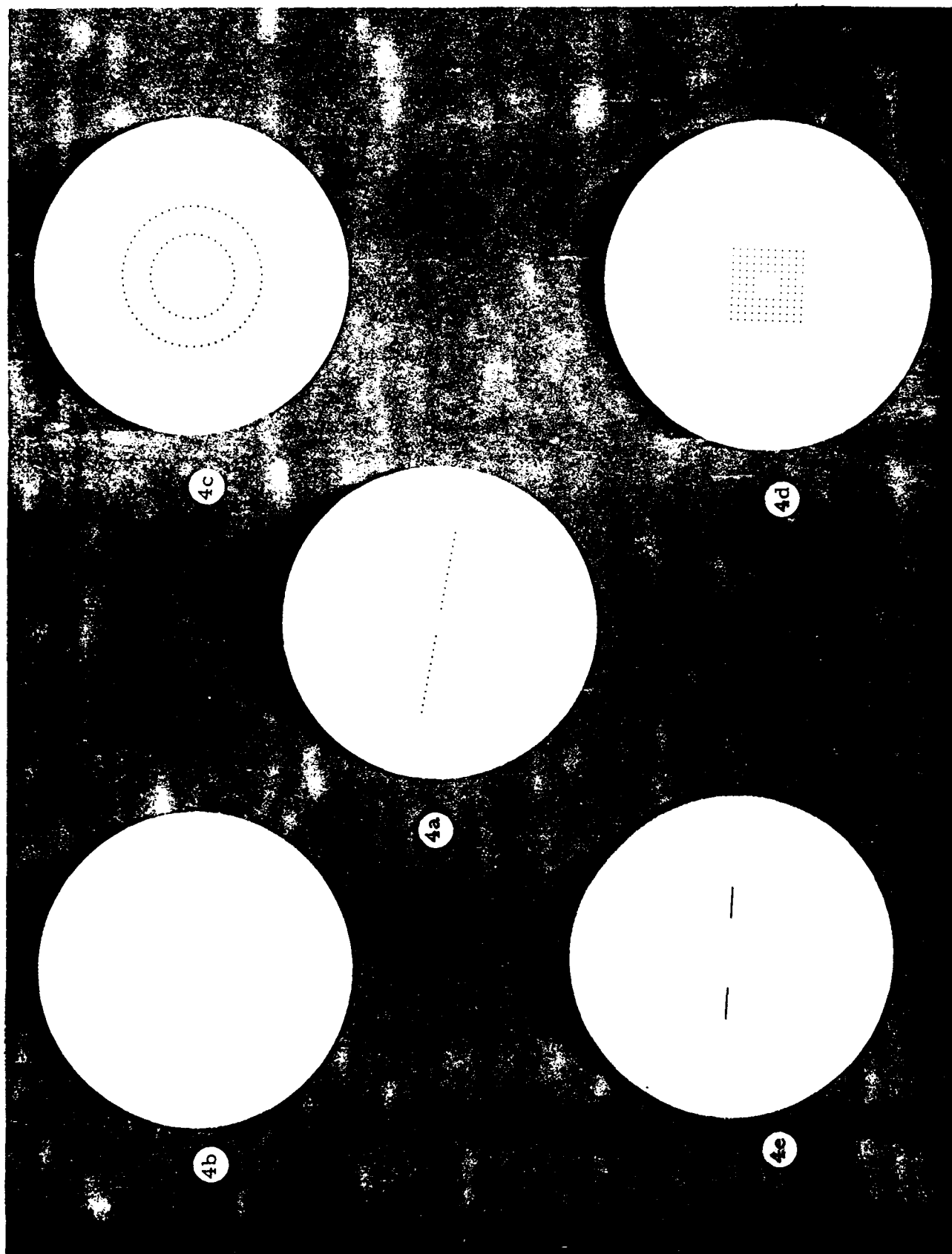
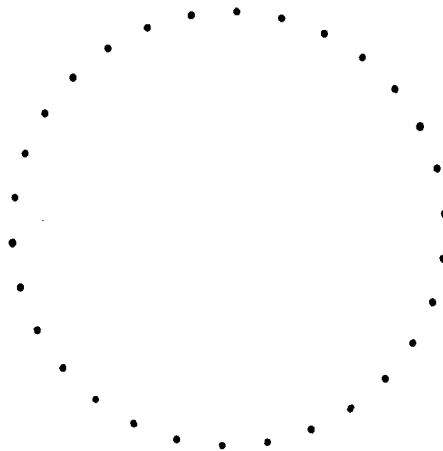


FIGURE 4. Contact Prints of Orifice Plates.

• • • • •

• • • • •

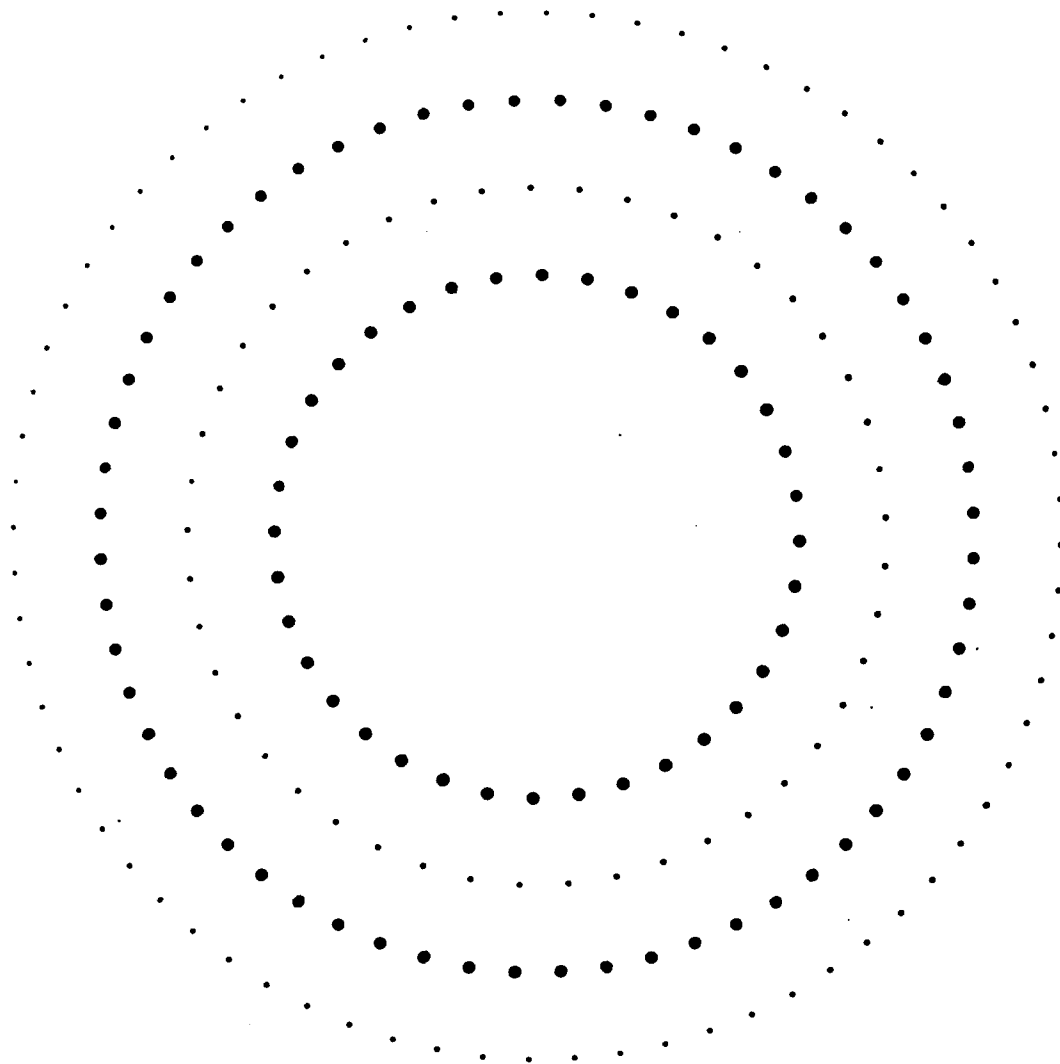
5a. Linear Array. 24 holes. 64 microns.



5b. Circular Array. 30 holes. 38 microns.

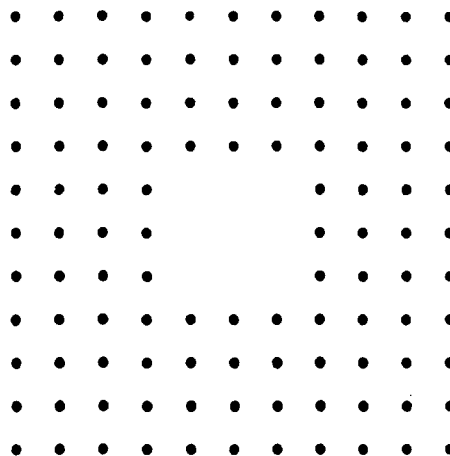
FIGURE 5. Projection Prints of Orifice Plates.





5c. Concentric Circular Array.  
117 holes. 38 microns.  
96 holes. 114 microns.

FIGURE 5. continued. Projection Prints of Orifice Plates.



5d. Rectangular Array. 112 holes. 76 microns.



5e. Slots.  
50.8 microns average width. 6350 microns long.

FIGURE 5. continued. Projection Prints of Orifice Plates.

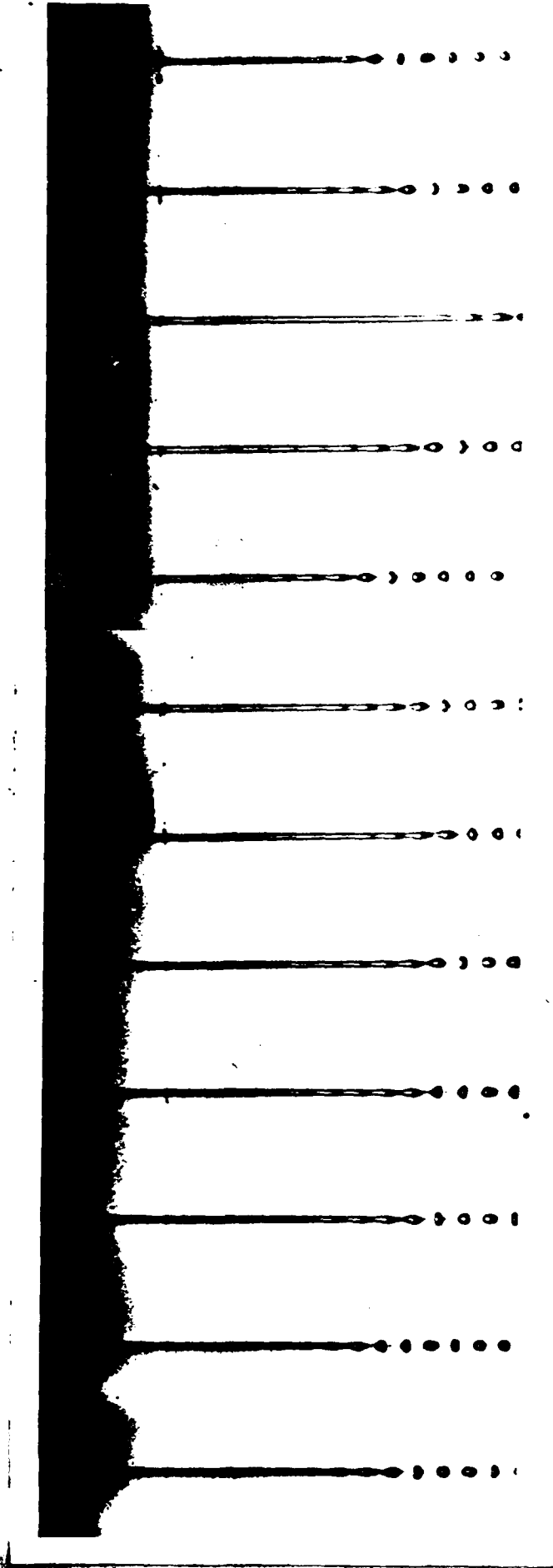


FIGURE 6a. Linear array positioned radially from stimulator. (Stimulator at left end of photo.)

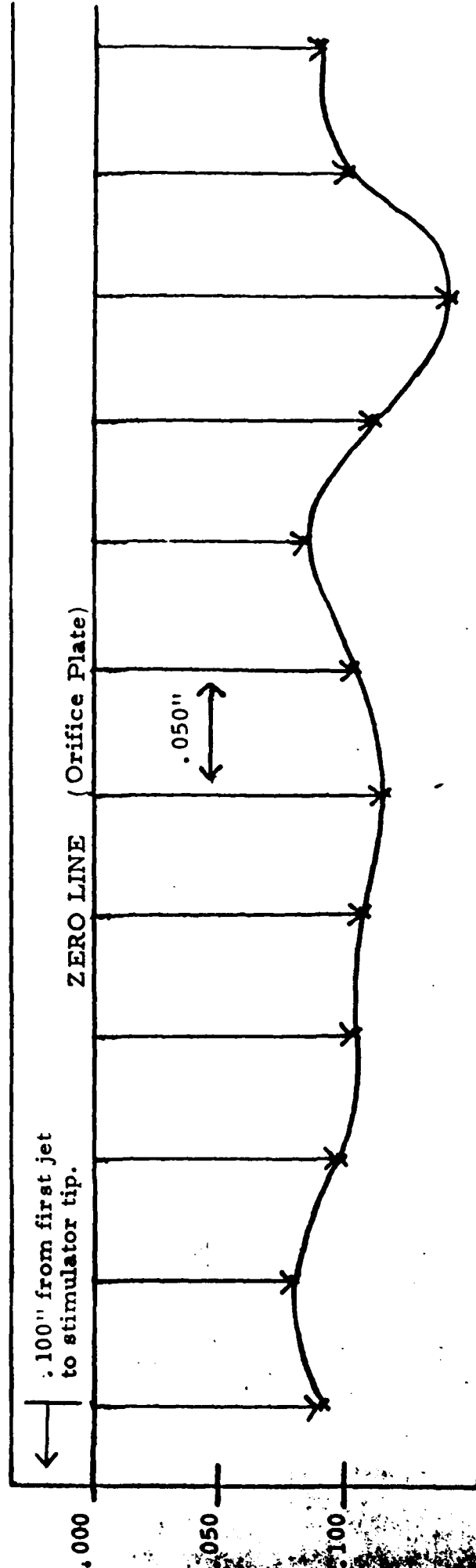


FIGURE 6b. Graphical representation of filament lengths shown in the photo above.

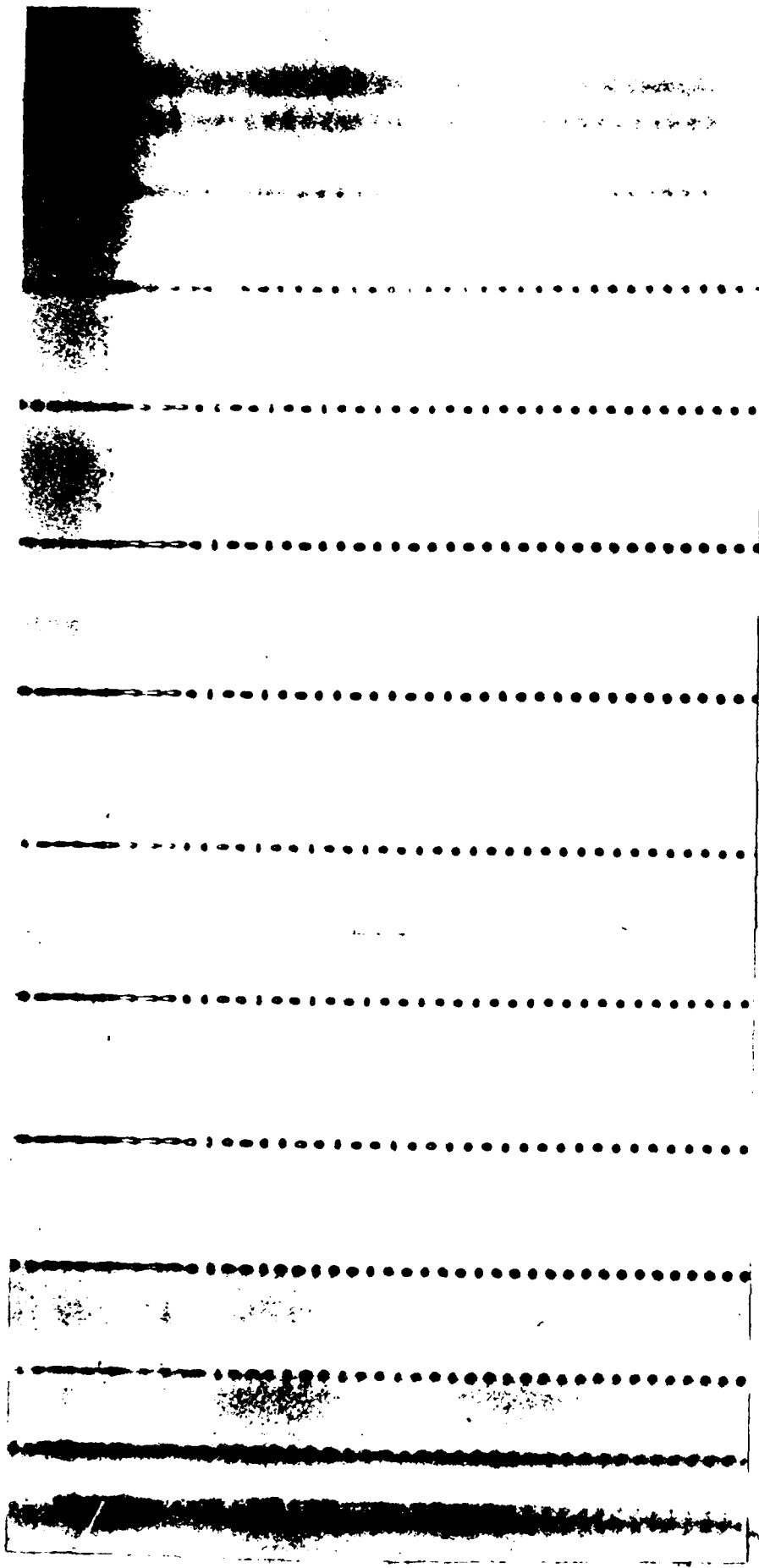


FIGURE 7.  
Circular Drop Array.  
30 jets. 70 micron drops.  
Composite Photo

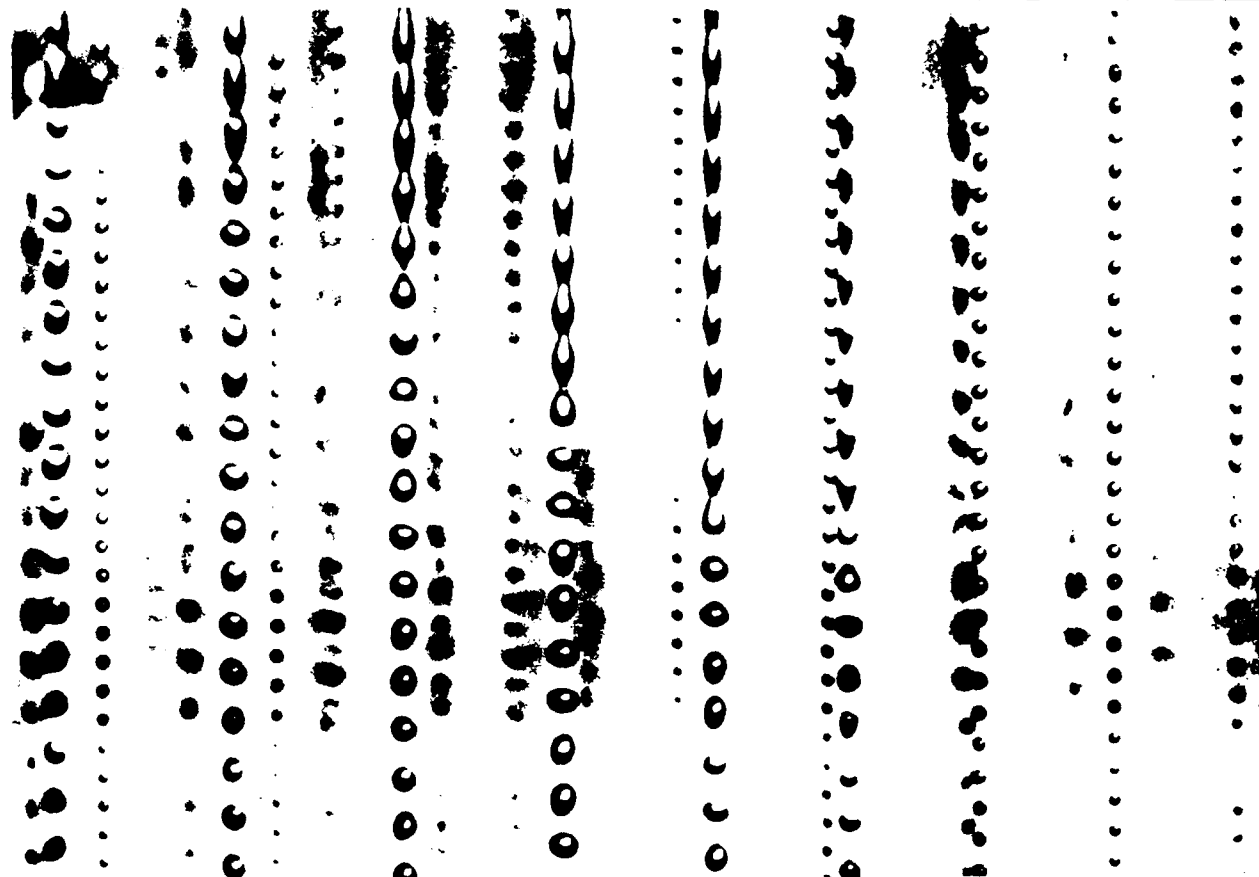


FIGURE 8. Array of 4 concentric circles.  
 117 jets with 70 micron drops.  
 96 jets with 120 micron drops.

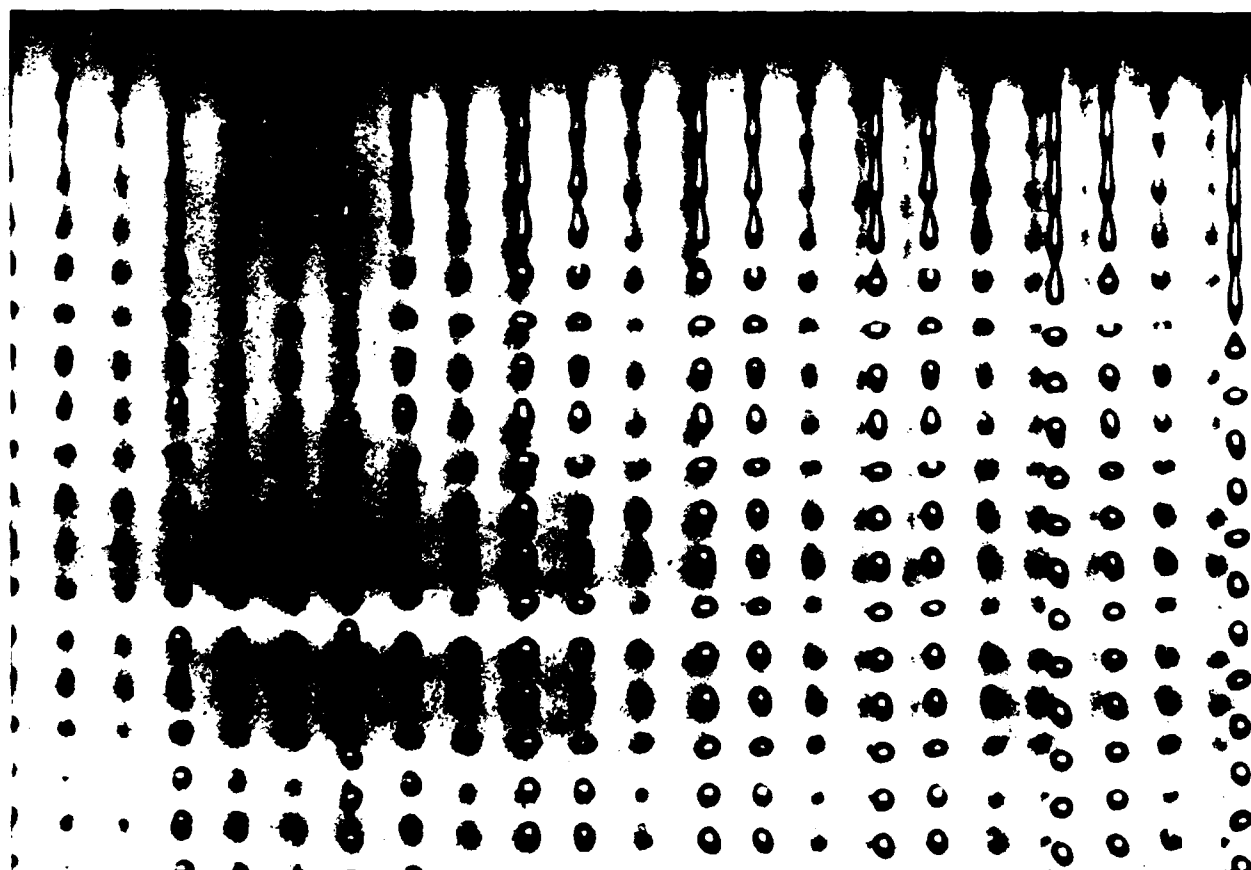


FIGURE 9. Rectangular Array. 112 jets. 150 micron drops.



FIGURE 10. Typical Rayleigh Break-up. 17.9 kHz.

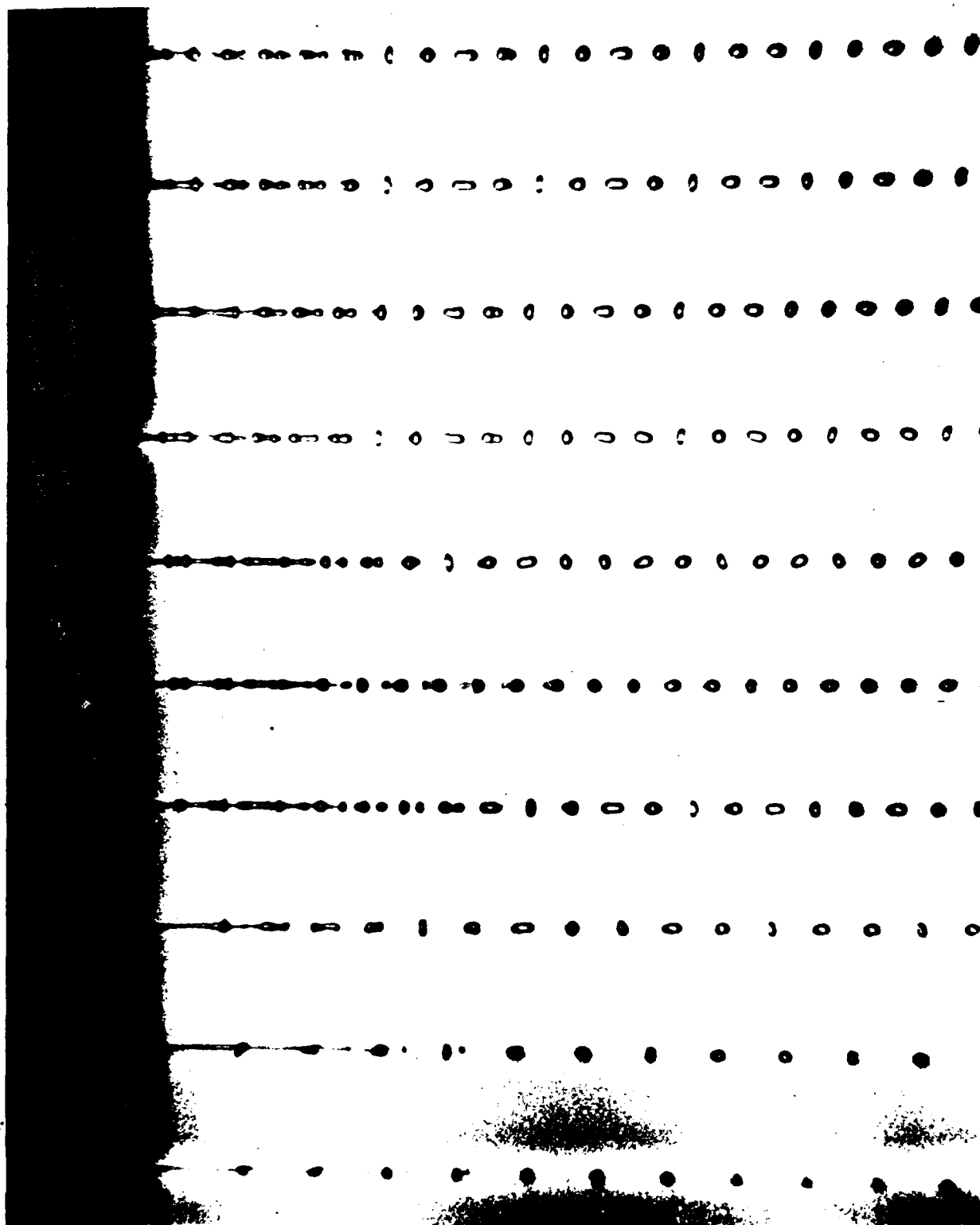


FIGURE 11. 17.9 kHz.  
Increased droplet spacing due to high amplitude stimulation.

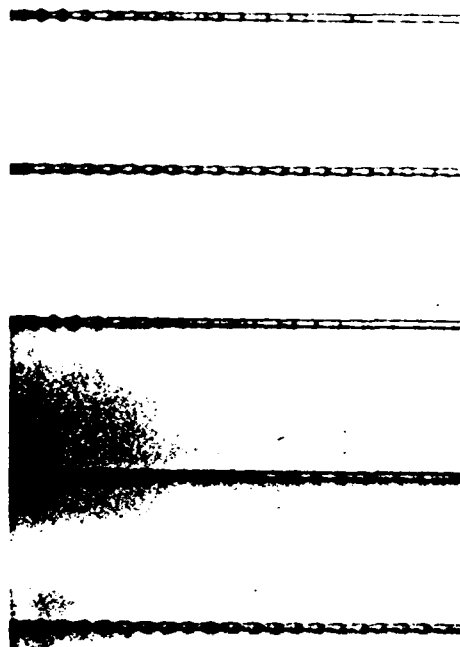


FIGURE 13a. Low Amplitude Stimulation.  
43.9 kHz. Stable Jets.

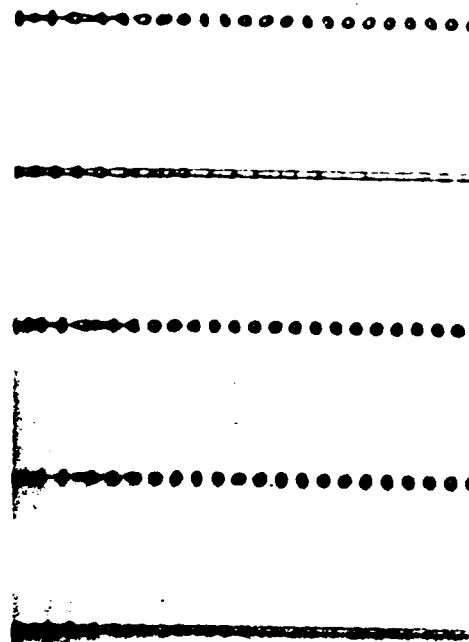


FIGURE 13b. High Amplitude Stimulation.  
43.9 kHz. Unstable Jets.

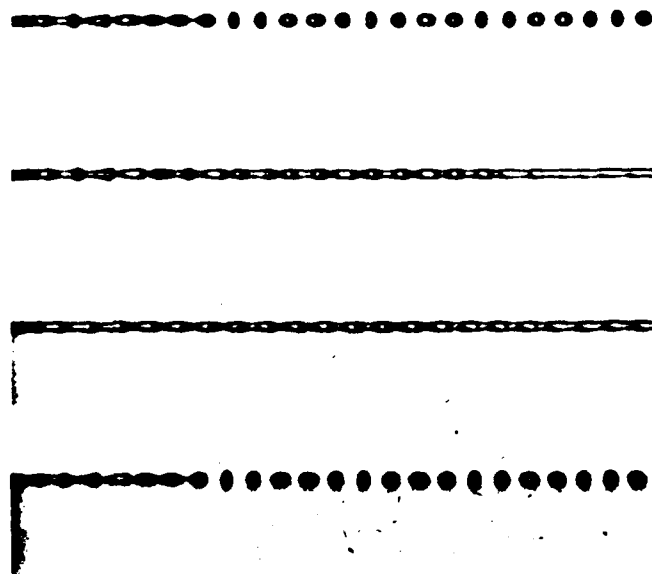
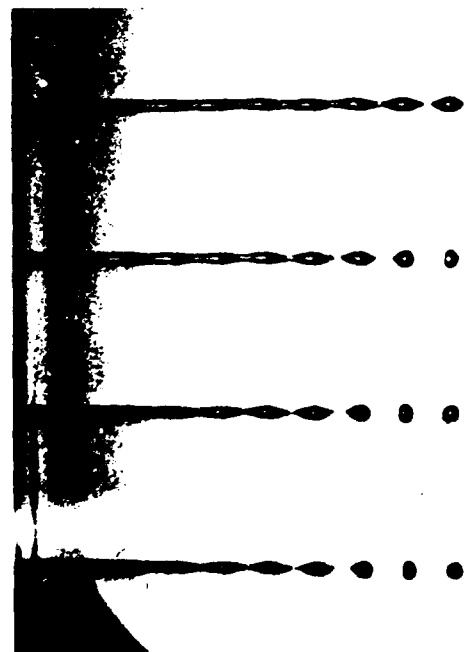


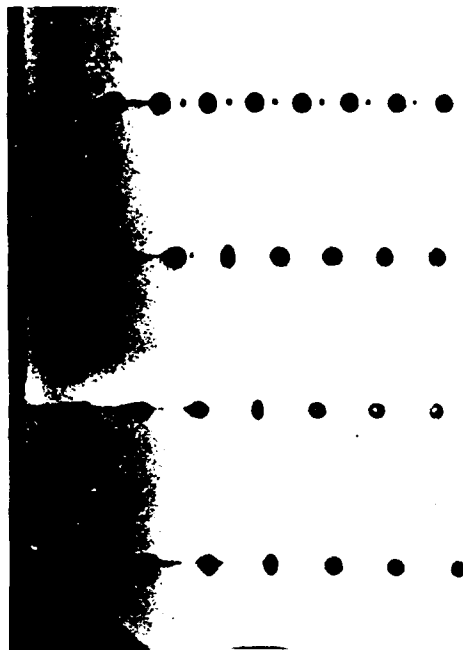
FIGURE 12. Amplitude Dependent  
Instabilities. 30.4 kHz.



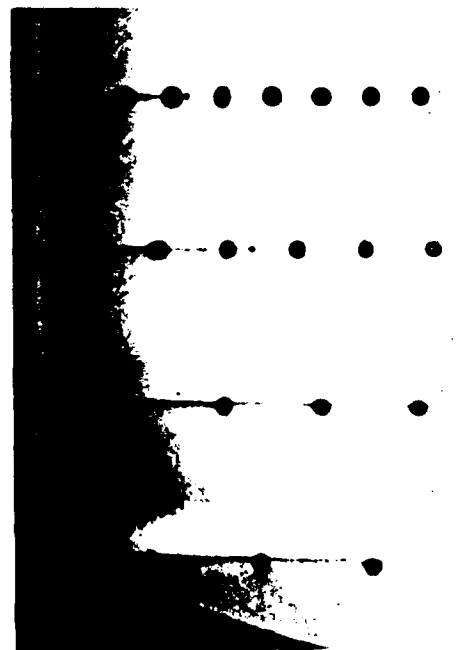
FIGURES 14 a-c. Droplet Spacing Stretching. 10 cp fluid.



14a. Low amplitude stimulation.  
15.4 kHz.



14b. Medium amplitude stimulation.  
15.4 kHz.



14c. High amplitude stimulation.  
15.4 kHz.

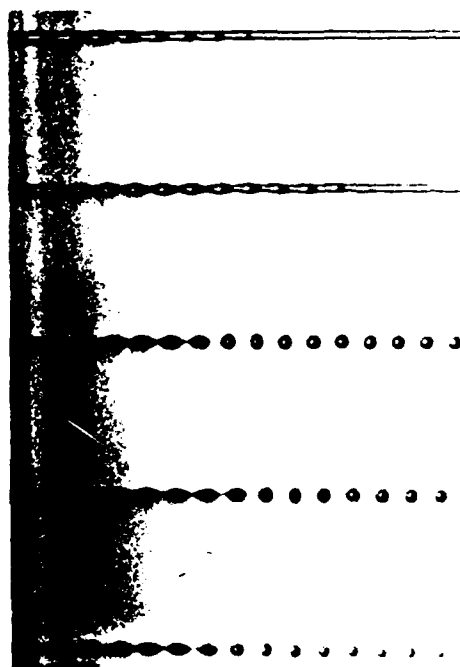


FIGURE 15. Amplitude dependent  
instability. 25.9 kHz. 10 cp fluid.

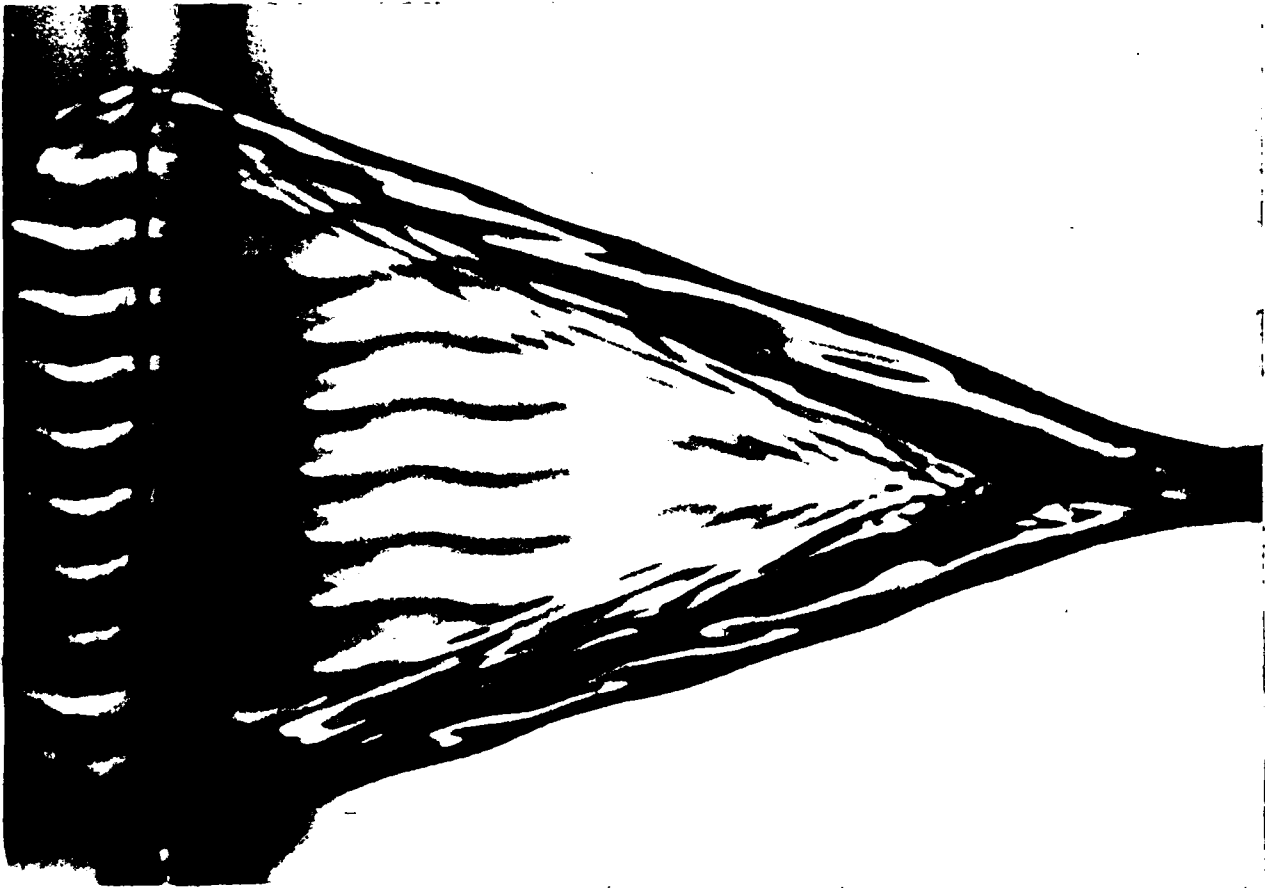


FIGURE 16a.  
Fluid sheet with spatial perturbations.

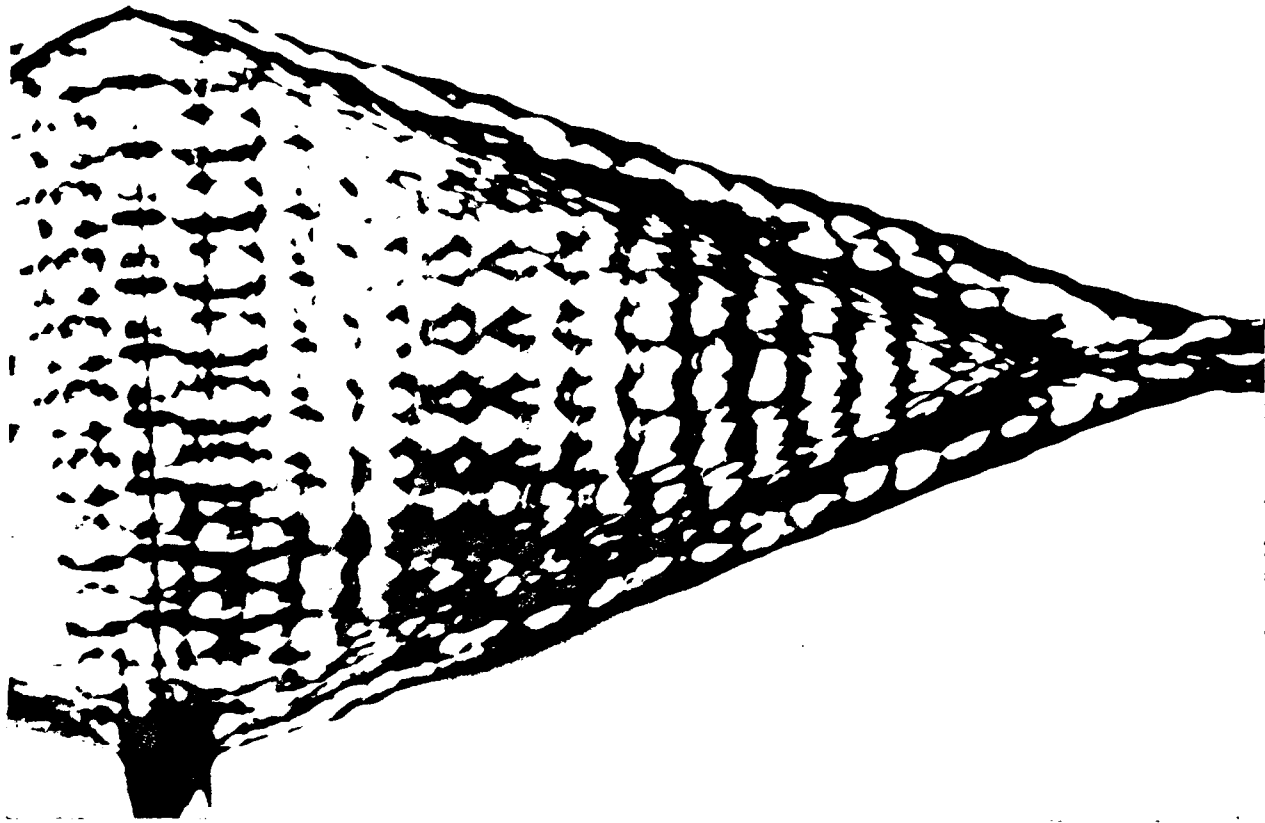


FIGURE 16b.  
Fluid sheet with spatial perturbations and  
sinusoidal velocity perturbations. 12.66 kHz

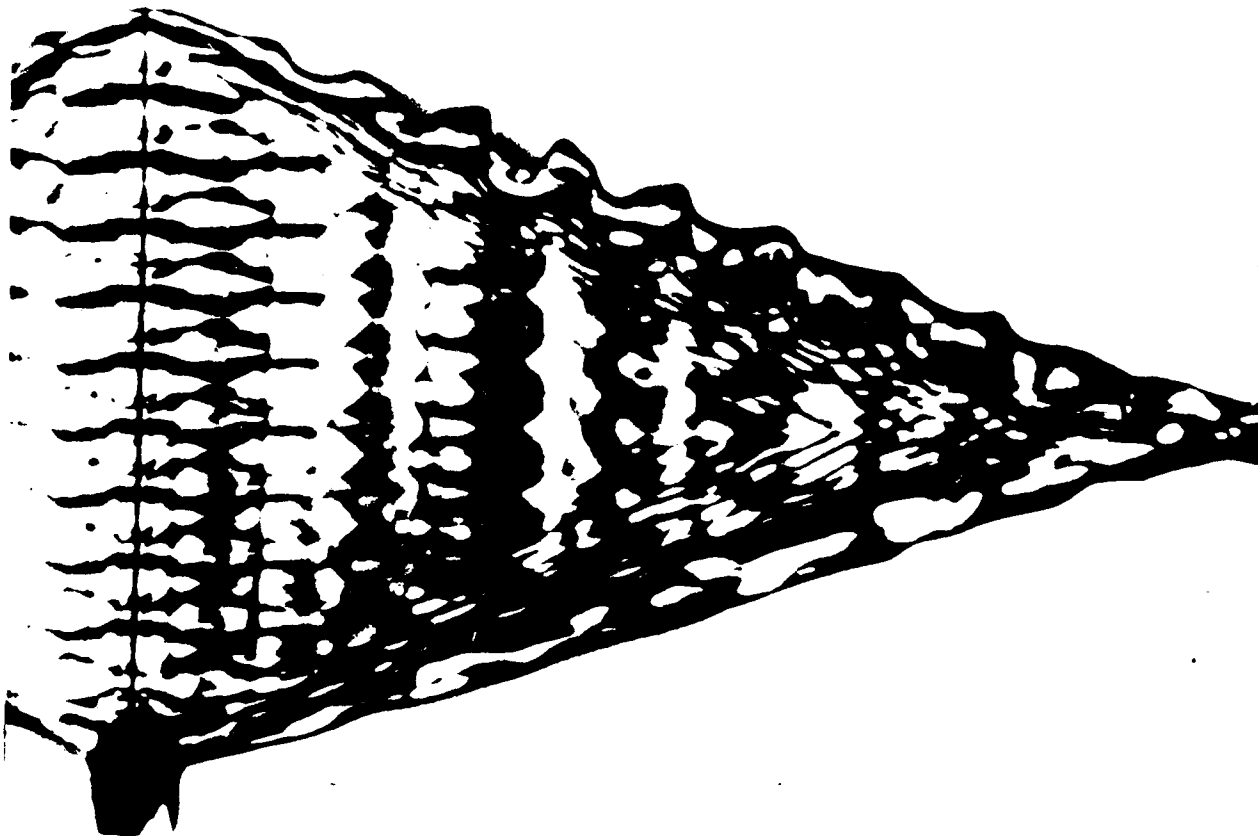


FIGURE 16c.

Fluid sheet with spatial perturbations and  
sinusoidal velocity perturbations. 5.46 kHz.

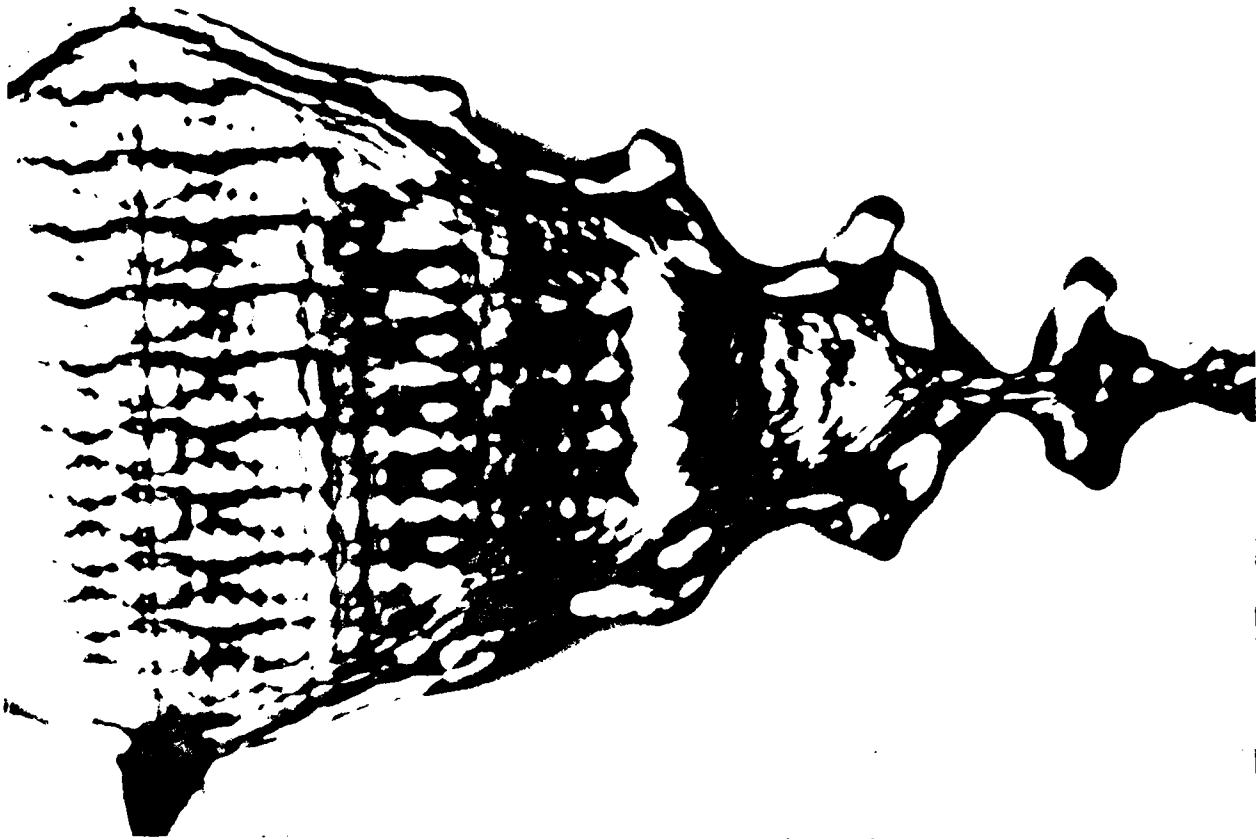


FIGURE 16d.

Fluid sheet with spatial perturbations and  
sinusoidal velocity perturbations. 2.50 kHz.

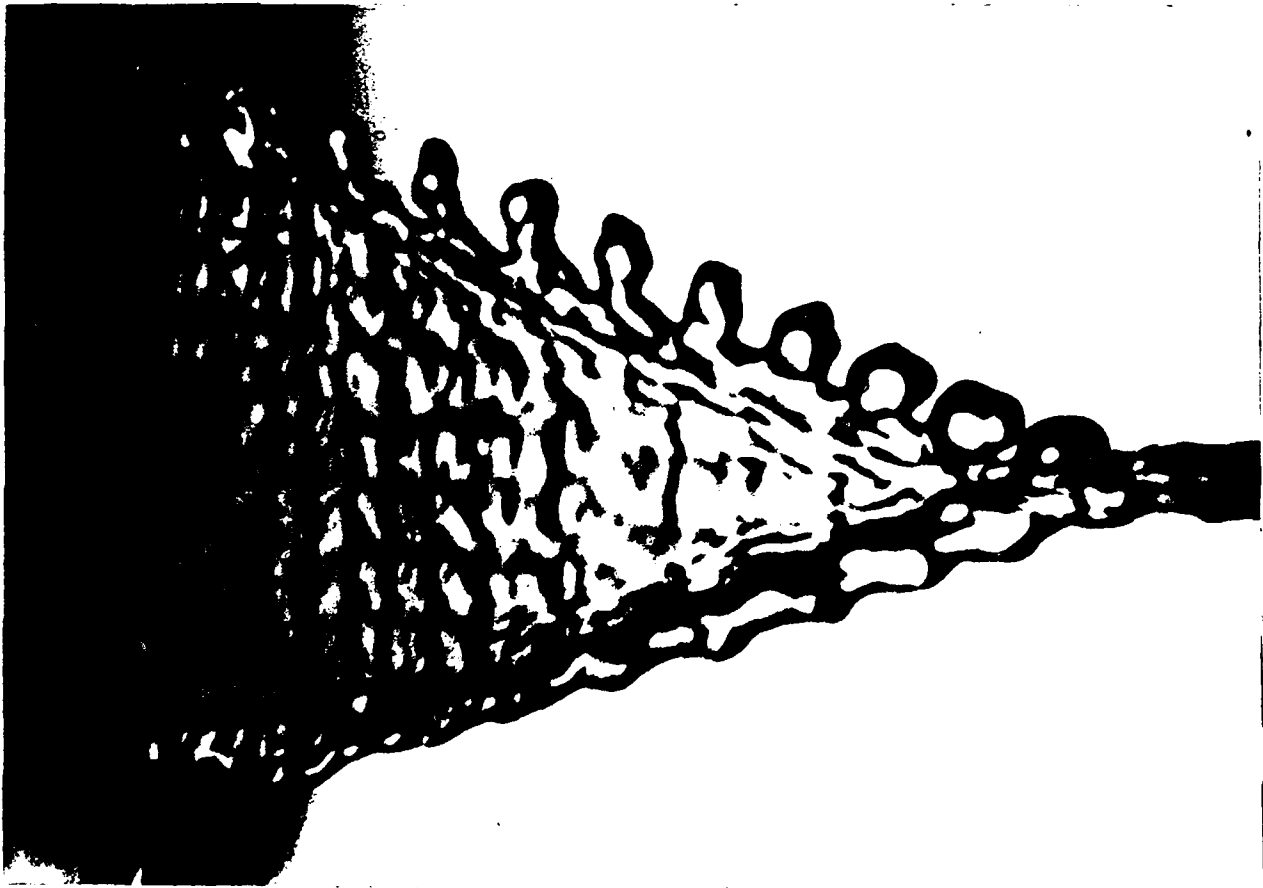


FIGURE 16e.  
Fluid sheet with spatial perturbations and  
square wave velocity perturbations. 5.5 kHz.

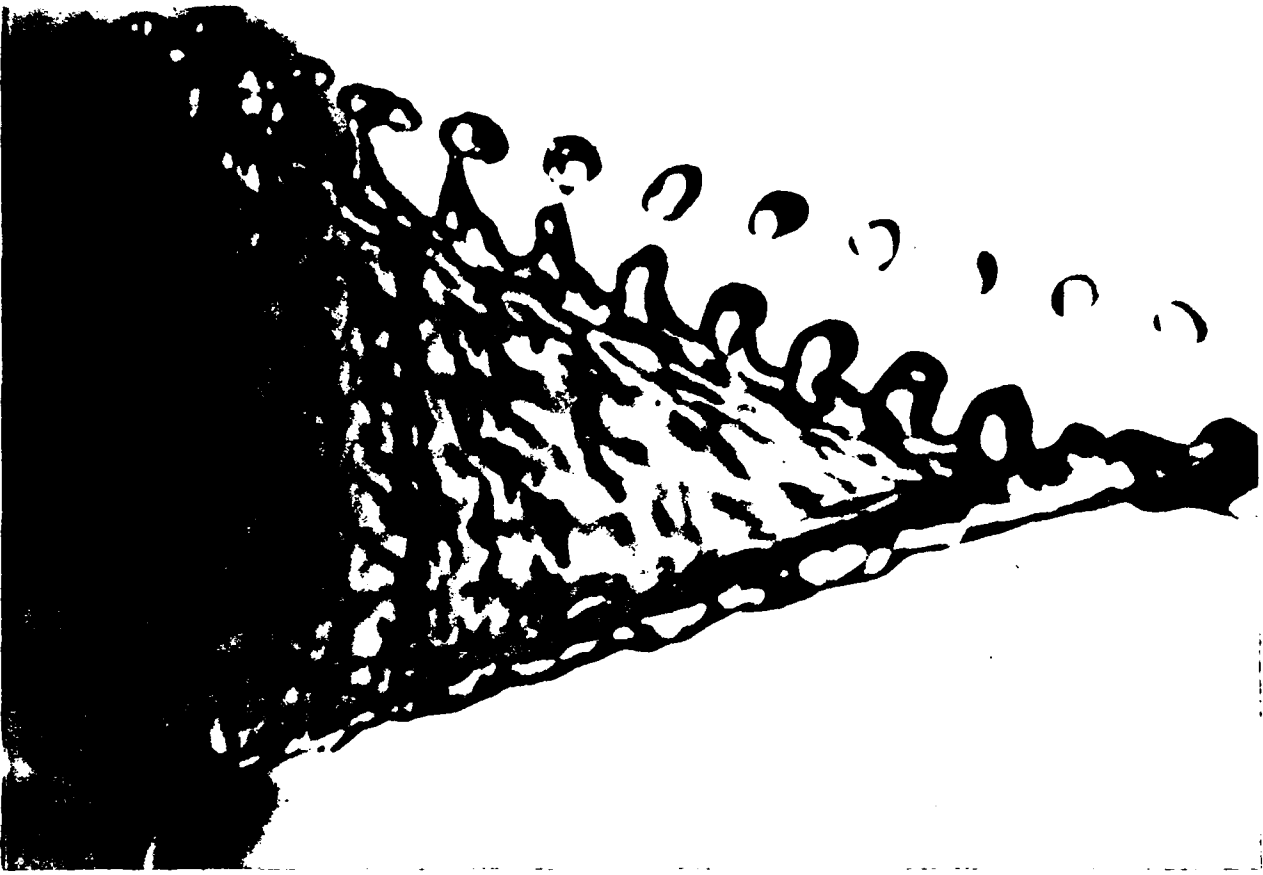


FIGURE 16f.  
Fluid sheet with spatial perturbations and  
square wave velocity perturbations. 5.5 kHz.  
Higher amplitude.

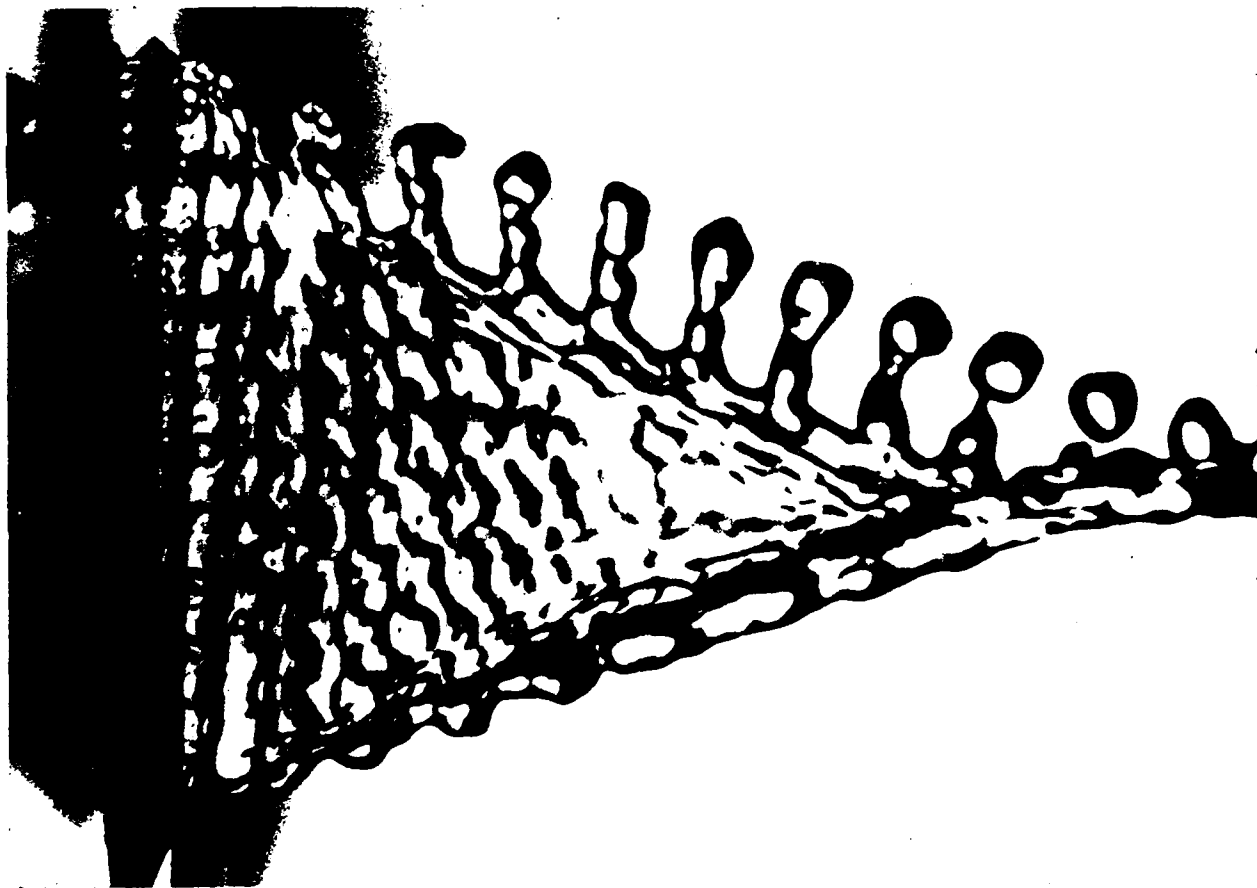
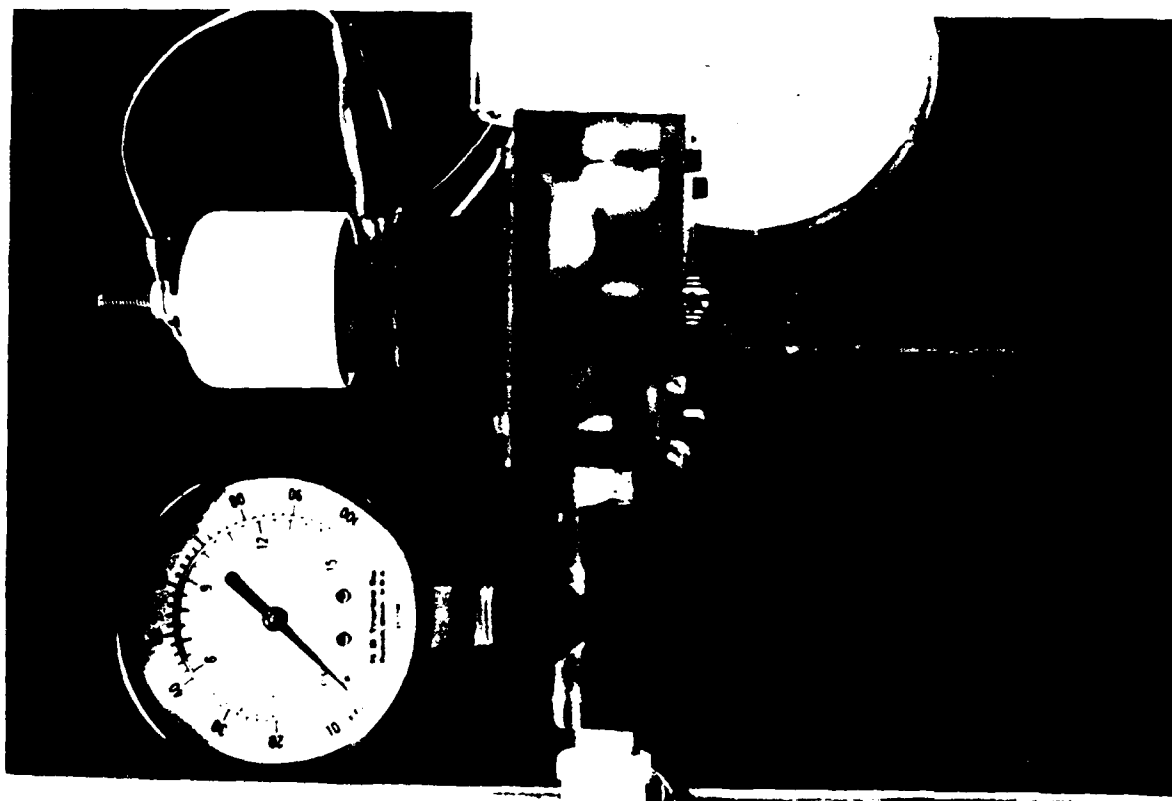
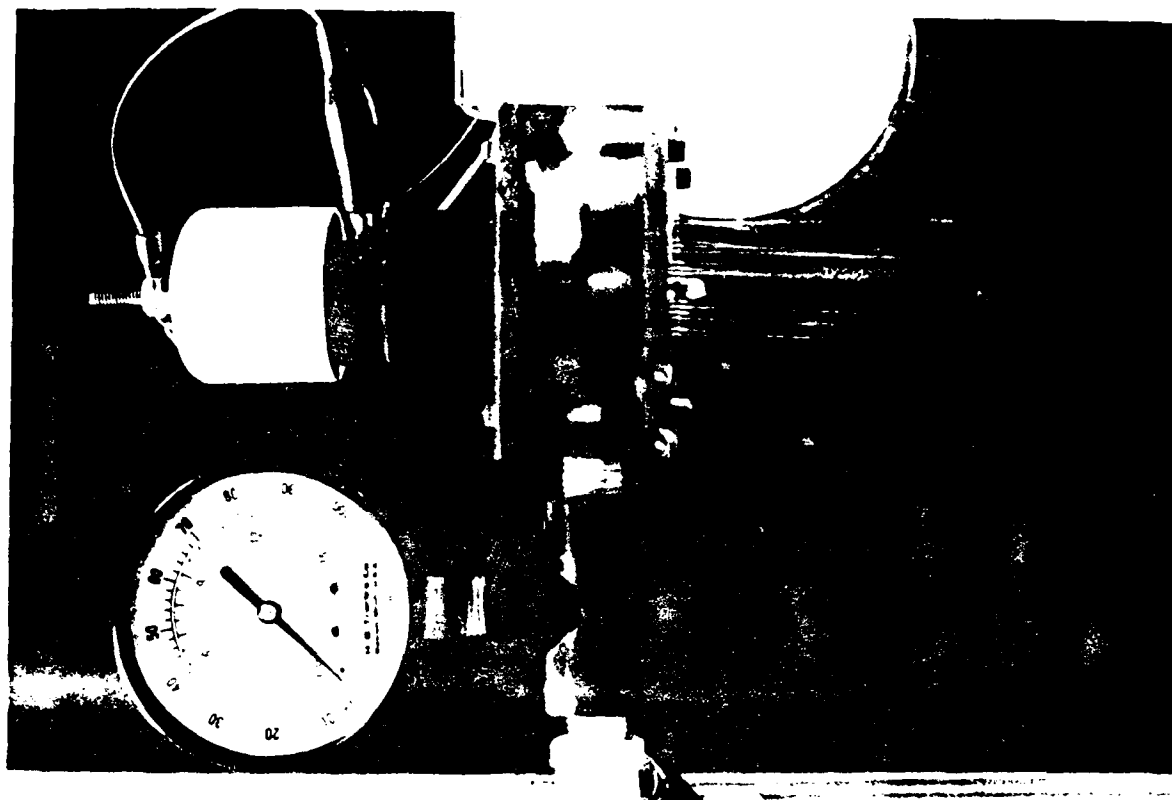


FIGURE 16g.  
Fluid sheet with spatial perturbations and  
square wave velocity perturbations. 5.0 kHz.



17a. Lower Amplitude Stimulation.



17b. Higher Amplitude Stimulation.

FIGURE 17. Acoustically Pumped Drop Streams. 10 cp. Fluid.